EC
Journals.ASM.org

Candida albicans VMA3 Is Necessary for V-ATPase Assembly and Function and Contributes to Secretion and Filamentation

Hallie S. Rane,[a] Stella M. Bernardo,[a,b] Summer M. Raines,[c] Jessica L. Binder,[c] Karlett J. Parra,[c] Samuel A. Lee[a,b]

Section of Infectious Diseases, New Mexico Veterans Healthcare System, Albuquerque, New Mexico, USA[a]; Division of Infectious Diseases, University of New Mexico Health Science Center, Albuquerque, New Mexico, USA[b]; Department of Biochemistry and Molecular Biology, University of New Mexico Health Science Center, Albuquerque, New Mexico, USA[c]

The vacuolar membrane ATPase (V-ATPase) is a protein complex that utilizes ATP hydrolysis to drive protons from the cytosol into the vacuolar lumen, acidifying the vacuole and modulating several key cellular response systems in *Saccharomyces cerevisiae*. To study the contribution of V-ATPase to the biology and virulence attributes of the opportunistic fungal pathogen *Candida albicans*, we created a conditional mutant in which *VMA3* was placed under the control of a tetracycline-regulated promoter (tetR-*VMA3* strain). Repression of *VMA3* in the tetR-*VMA3* strain prevents V-ATPase assembly at the vacuolar membrane and reduces concanamycin A-sensitive ATPase-specific activity and proton transport by more than 90%. Loss of *C. albicans* V-ATPase activity alkalinizes the vacuolar lumen and has pleiotropic effects, including pH-dependent growth, calcium sensitivity, and cold sensitivity. The tetR-*VMA3* strain also displays abnormal vacuolar morphology, indicative of defective vacuolar membrane fission. The tetR-*VMA3* strain has impaired aspartyl protease and lipase secretion, as well as attenuated virulence in an *in vitro* macrophage killing model. Repression of *VMA3* suppresses filamentation, and V-ATPase-dependent filamentation defects are not rescued by overexpression of *RIM8*, *MDS3*, *EFG1*, *CST20*, or *UME6*, which encode positive regulators of filamentation. Specific chemical inhibition of Vma3p function also results in defective filamentation. These findings suggest either that V-ATPase functions downstream of these transcriptional regulators or that V-ATPase function during filamentation involves independent mechanisms and alternative signaling pathways. Taken together, these data indicate that V-ATPase activity is a fundamental requirement for several key virulence-associated traits in *C. albicans*.

Candida albicans is a major opportunistic human fungal pathogen and is responsible for 6.8% of hospital-acquired infections in the United States (1). Despite the availability of several classes of antifungal drugs, attributable mortality, cost of care, and length of stay due to invasive candidiasis remain unacceptably high (2, 3). In addition, resistance to currently available antifungal drugs is emerging (see reference 4 for a review). Therefore, development of new antifungal drug targets remains a critical need. A diverse set of factors contributing to *C. albicans* virulence have been identified, including the secretion of aspartyl proteases and lipases, filamentation, and biofilm formation (5–8). Understanding the biology and regulation of these processes and pathways may illuminate new candidates for antifungal therapy.

The vacuole is a dynamic acidic organelle found in yeast and plants that is analogous to the mammalian lysosome. It functions in an array of cellular homeostasis processes and thereby plays an important role in stress response, adaptation to novel environments, and cell differentiation (9–13). Furthermore, in *C. albicans*, intact vacuolar function is important for filamentation and virulence (12–15). Vacuolar function depends on the maintenance of acidic pH by the vacuolar H-ATPase (V-ATPase), an enzyme complex that functions in organelle acidification across eukaryotes (16, 17). The V-ATPase utilizes hydrolysis of ATP to transport protons from the cytosol into a variety of organelles. V-ATPase-mediated acidification and membrane energization are necessary for important vacuolar functions, including calcium and metal homeostasis (18), cargo sorting and membrane trafficking in endocytic and secretory pathways (19), and drug resistance (20). In *Saccharomyces cerevisiae*, the V-ATPase is expressed at the vacuolar membrane and the membrane of prevacuolar compartments and the Golgi compartment.

The V-ATPase complex consists of the V_1 and V_o subcomplexes (16). The V_1 subcomplex is composed of peripherally associated subunits that form the sites of ATP binding and hydrolysis on the cytosolic side of the membrane. The V_o subcomplex spans the vacuolar membrane and mediates transport of protons from the cytosol to vacuolar the lumen. Rotation of V_1 and V_o subunits relative to the catalytic sites couples ATP hydrolysis and active transport of protons across the vacuolar membrane (16). By driving protons into the vacuole, V-ATPase generates an acidic luminal pH (pH ~6.25) required for proper activity of various degradative vacuolar enzymes (21) and a membrane potential that energizes secondary transport systems (17, 22). Loss of V-ATPase function in *S. cerevisiae* leads to a set of growth defects referred to collectively as the *vma* phenotype. The *vma* phenotype is characterized by the inability to grow on media that are alkaline (pH 7.5 to 8.5), contain high concentrations of calcium, or contain nonfermentable carbon sources as the sole carbon source (16), whereas growth on acidic media (pH 4.0 to 5.0) is similar to that of the wild type. Thus, interruption of V-ATPase function interferes with a variety of key cellular processes and stress responses likely important for fungal virulence; however, little is known

Received 15 May 2013 **Accepted** 30 July 2013
Published ahead of print 2 August 2013
Address correspondence to Samuel A. Lee, SamALee@salud.unm.edu.
Supplemental material for this article may be found at http://dx.doi.org/10.1128/EC.00118-13.

doi:10.1128/EC.00118-13

regarding the specific functions of the V-ATPase complex in *C. albicans* (17).

In *S. cerevisiae*, the *VMA3* gene encodes the c subunit of the V_o subcomplex. The c subunit forms a hexameric ring with the c′ and c″ subunits of the V-ATPase, which are encoded by *VMA11* and *VMA16*, respectively. This hexameric ring is the main site of proton transport by the V-ATPase complex. *VMA3*, *VMA11*, and *VMA16* each encode hydrophobic proteins with four or five transmembrane domains. Proton transport from the cytosol to negatively charged glutamic acid residues in the c ring involves V_o subunit a (V_oa) (17, 23). The V_oa subunit is the only fungal V-ATPase subunit encoded by two isoforms, *VPH1* and *STV1*. We have recently shown that V-ATPase pumps containing Vph1p versus Stv1p contribute differently to *C. albicans* cell biology and virulence-related traits (24). Whereas *C. albicans VMA3* has not been previously studied, loss-of-function mutations in the *VMA3* gene have been investigated extensively in *S. cerevisiae* (25–28) and result in pleiotropic effects, including vacuolar alkalinization, impaired disassembly of the V_o and V_1V_o complexes (28), and the *vma* growth phenotype (26).

In this study, we generated a *C. albicans* tetracycline-regulatable *VMA3* mutant(tetR-*VMA3* strain) in order to analyze the contribution of *VMA3* to V-ATPase function, vacuolar morphology, and virulence-related phenotypes. Importantly, we demonstrate that the V-ATPase plays a central role in the induction of *C. albicans* filamentation; Vma3p-dependent filamentation defects are dominant and independent of several well-characterized filamentation and pH-responsive signaling pathways.

MATERIALS AND METHODS

Identification of Vma3p. A single potential ortholog of *S. cerevisiae* Vma3p (http://www.yeastgenome.org/) was identified by a BLASTp search of the Candida Genome Database (http://www.candidagenome.org/). The resulting sequence (orf19.5886) was aligned with that of *S. cerevisiae* Vma3p using the software program MAFFT (29). The alignment was used as a query in the program PRALINE to analyze protein conservation, hydrophobicity, and transmembrane structure (30).

Strains and media. Strains used in this study are listed in Table 1. Throughout, unbuffered medium is used to refer to any growth medium where no buffering agents were added to maintain the pH of the medium. For testing of specific pH-dependent phenotypes, medium was buffered to pH 4.0 or 5.0 using 50 mM succinic acid–50 mM Na_2PO_4 or to pH 7.5 or 8.5 using 50 mM morpholineethanesulfonic acid (MES) hydrate–50 mM morpholinepropanesulfonic acid (MOPS). Standard growth was completed at 30°C in unbuffered yeast peptone dextrose (YPD) (1% yeast extract, 2% peptone, and 2% glucose) supplemented with 80 μg/ml uridine where required. Doxycycline was added to a final concentration of 20 μg/ml when needed. For all experiments, cells were inoculated overnight in unbuffered YPD and then reset in fresh unbuffered YPD with and without doxycycline and grown for 24 h at 30°C with shaking in order to completely repress *VMA3* expression prior to the start of the experiment.

Attempted disruption of *VMA3*. Primers used in this study are indicated in Table 2. We first attempted to generate a *VMA3* null mutant in *C. albicans* using a PCR-based gene disruption strategy (31). The primers *VMA3*-5DRb and *VMA3*-3DRb were used to amplify the *dpl200-URA3-dpl200*-containing plasmid pDDB57 (from A. Mitchell, Carnegie Mellon University). Transformation of *C. albicans* BWP17 with the *vma3*Δ::*dpl200-URA3-dpl200* PCR amplicon was performed using the lithium acetate method. Because *S. cerevisiae vma* mutants exhibit poor growth at alkaline pH, selective medium was buffered to pH 4.0 or 5.0 to facilitate disruption of the second *VMA3* allele. Genomic DNA was extracted from transformants as described previously (32). The transformants were screened for homologous reintegration via PCR using primers *VMA3*-5Det and *VMA3*-3Det. Disruption of the second allele of *VMA3* was attempted using the *VMA3*-5DRb and *VMA3*-3DRb primers to amplify the plasmid pRS-ARG4ΔSpeI (from A. Mitchell, Carnegie Mellon University) (33). This *vma3*Δ::*ARG4* PCR amplicon was used to transform *C. albicans VMA3/vma3*Δ::*dpl200-URA3-dpl200* mutants via the lithium acetate method and plated to selective medium without arginine buffered to pH 4.0 or 5.0. The genotype of the resulting mutants was assessed by allele-specific PCR using the primers *VMA3*-5Det and *VMA3*-3Det.

Construction of a tetracycline-regulated *VMA3* gene. One *C. albicans VMA3* allele was deleted from the THE1 strain background using PCR-based gene disruption (31) and transformation via the lithium acetate method. The primers *VMA3*-5DRb and *VMA3*-3DRb (Table 2) were used to amplify the plasmid pDDB57. Strain THE1 was transformed with the resulting PCR amplicon to generate strain *VMA3*Δ/+ (Table 1). Correct genomic integration of the gene disruption cassette was confirmed via PCR using the primers *VMA3*-5Det and *VMA3*-3Det. Then, the *VMA3*Δ/+ strain was plated to fluoroorotic acid (FOA) agar medium, and the resultant FOA-resistant colonies were screened via PCR for the *VMA3/vma3*Δ::*dpl200* genotype using the primers *VMA3*-5Det and *VMA3*-3Det. The tetracycline-regulatable system described by Nakayama et al. (34), with modifications allowing PCR-directed targeting as described by Bates et al. (35), was used to place the remaining *VMA3* allele under a tetracycline-regulatable promoter. The primers tet*VMA3*-5DR and tet*VMA3*-3DR were used to amplify plasmid p99CAU1 (H. Nakayama, Suzuka University) using the primer design strategy described by Bates et al. (35). This PCR amplicon was inserted upstream of the remaining *VMA3* allele of the *VMA3*Δ/+ FOA strain via lithium acetate transformation. Transformants were screened for correct insertion of the tetR-*VMA3* allele using the primers tet*VMA3*-5Det and tet*VMA3*-3Det. Expression of *VMA3* in the THE1-CIp10 control strain and the tetR-*VMA3* strain after 24 h of growth in unbuffered YPD with or without doxycycline was assayed using reverse transcriptase PCR (RT-PCR). RT-PCR was performed using the Access RT-PCR system (Promega) according to the manufacturer's instructions and using the primers RT-*VMA3*-5Det and RT-*VMA3*-3Det and 5 μg total mRNA as the template. Absence of contaminating DNA was tested in parallel PCR-based reactions. The correct genotype of these strains was confirmed by Southern blotting following standard protocols (36). In brief, genomic DNA prepared from candidate strains was digested with XhoI (New England BioLabs) and run on a 0.6% (wt/vol) agarose gel. A digoxigenin-labeled probe (nucleotide [nt] −800 to nt 500 of orf19.5886) was prepared from genomic DNA isolated from strain THE1 with the primers *VMA3*-5Sblt and *VMA3*-3Sblt (Table 2) and reagents supplied in the PCR DIG probe synthesis kit (Roche).

Growth at various pHs. The ability of strains to grow on medium without a pH buffer was tested on unbuffered YPD and unbuffered complete synthetic medium (CSM) (0.67% yeast nitrogen base without amino acids [YNB], 0.079% complete synthetic mixture, 2% glucose, and 2% agar) with or without doxycycline added. The ability of strains to grow over a pH range was tested on CSM buffered to pH 4.0 to 8.5 with or without doxycycline added. Cells from overnight cultures were washed and counted as previously described (37). Phosphate-buffered saline (PBS) was inoculated with cells from overnight cultures to a starting density of 10^8 cells/ml. Then, a total of five 5-fold dilutions were completed in 96-well plates, and cells were stamped onto agar plates using a multiblot replicator (VP 408H; VP Scientific) and incubated at 30°C for 48 h. Growth at pH 4.0 to 8.5 was also tested in liquid medium: cells from overnight cultures were diluted to an optical density at 600 nm (OD_{600}) of 0.05 in CSM buffered to pH 4.0 to 8.5 and with or without doxycycline added. Then, cells were grown at 30°C using a Biotek Synergy H1M instrument with double orbital shaking at fast speed and 2-mm frequency, with OD_{600} readings taken at 15-min intervals.

Stress response. The ability of the tetR-*VMA3* strain to grow on media containing various stressors was tested on agar plates with and without

TABLE 1 *C. albicans* strains used in this study

Strain name or description	Parent strain or description	Relevant genotype[a]	Source or reference
BWP17	SC5314	*ura3Δ/ura3Δ arg4Δ/arg4Δ hisΔ/his1Δ VMA3/VMA3*	Wilson et al. 1999 (33)
BWP17-*VMA3*Δ/+	BWP17	*ura3Δ/ura3Δ arg4Δ/arg4Δ hisΔ/his1Δ VMA3/vma3Δ::dpl200-URA3-dpl200*	This study
THE1	CAI8	*ade2Δ::hisG/ade2Δ::hisG ura3Δ::imm434/ura3Δ::imm434 ENO1/eno1Δ::ENO1*-tetR-ScHAP4AD-3×HA-*ADE2 VMA3/VMA3*	Nakayama et al. 2000 (34)
THE1-CIp10	THE1	*ade2Δ::hisG/ade2Δ::hisG ura3Δ::imm434/ura3Δ::imm434 ENO1/eno1Δ::ENO1*-tetR-ScHAP4AD-3×HA-*ADE2 RP10/RP10::URA3 VMA3/VMA3*	Bernardo et al. 2008 (14)
*vma3*Δ/+ strain	THE1	*ura3Δ::imm434/ura3Δ::imm434 VMA3/vma3Δ::dpl200-URA3-dpl200 ade2Δ::hisG/ade2Δ::hisG ura3Δ::imm434/ura3Δ::imm434 ENO1/eno1Δ::ENO1*-tetR-ScHAP4AD-3×HA-*ADE2*	This study
*vma3*Δ/+ FOA strain	*VMA3*Δ/+ strain	*ura3Δ::imm434/ura3Δ::imm434 VMA3/vma3Δ::dpl200 ade2Δ::hisG/ade2Δ::hisG ura3Δ::imm434/ura3Δ::imm434 ENO1/eno1Δ::ENO1*-tetR-ScHAP4AD-3×HA-*ADE2*	This study
tetR-*VMA3* strain	*VMA3*Δ/+ FOA strain	*ura3Δ::imm434/ura3Δ::imm434 vma3Δ::dpl200*::99t-*VMA3-URA3 ade2Δ::hisG/ade2Δ::hisG ura3Δ::imm434/ura3Δ::imm434 ENO1/eno1Δ::ENO1*-tetR-ScHAP4AD-3×HA-*ADE2*	This study
tetR-*VMA3*+*NAT1-*P_{ENO1}*-RIM8* strain	tetR-*VMA3* strain	*ura3Δ::imm434/ura3Δ::imm434 vma3Δ::dpl200*::99t-*VMA3-URA3 ade2Δ::hisG/ade2Δ::hisG ura3Δ::imm434/ura3Δ::imm434 ENO1/eno1Δ::ENO1*-tetR-ScHAP4AD-3×HA-*ADE2 NAT1-*P_{ENO1}*-RIM8/RIM8*	This study
tetR-*VMA3*+*NAT1-*P_{ENO1}*-MDS3* strain	tetR-*VMA3* strain	*ura3Δ::imm434/ura3Δ::imm434 vma3Δ::dpl200*::99t-*VMA3-URA3 ade2Δ::hisG/ade2Δ::hisG ura3Δ::imm434/ura3Δ::imm434 ENO1/eno1Δ::ENO1*-tetR-ScHAP4AD-3×HA-*ADE2 NAT1-*P_{ENO1}*-MDS3/MDS3*	This study
tetR-*VMA3*+*NAT1-*P_{ENO1}*-UME6* strain	tetR-*VMA3* strain	*ura3Δ::imm434/ura3Δ::imm434 vma3Δ::dpl200*::99t-*VMA3-URA3 ade2Δ::hisG/ade2Δ::hisG ura3Δ::imm434/ura3Δ::imm434 ENO1/eno1Δ::ENO1*-tetR-ScHAP4AD-3×HA-*ADE2 NAT1-*P_{ENO1}*-UME6/UME6*	This study
tetR-*VMA3*+*NAT1-*P_{ENO1}*-EFG1* strain	tetR-*VMA3* strain	*ura3Δ::imm434/ura3Δ::imm434 vma3Δ::dpl200*::99t-*VMA3-URA3 ade2Δ::hisG/ade2Δ::hisG ura3Δ::imm434/ura3Δ::imm434 ENO1/eno1Δ::ENO1*-tetR-ScHAP4AD-3×HA-*ADE2 NAT1-*P_{ENO1}*-EFG1/EFG1*	This study
tetR-*VMA3*+*NAT1-*P_{ENO1}*-CST20* strain	tetR-*VMA3* strain	*ura3Δ::imm434/ura3Δ::imm434 vma3Δ::dpl200*::99t-*VMA3-URA3 ade2Δ::hisG/ade2Δ::hisG ura3Δ::imm434/ura3Δ::imm434 ENO1/eno1Δ::ENO1*-tetR-ScHAP4AD-3×HA-*ADE2 NAT1-*P_{ENO1}*-CST20/CST20*	This study

[a] HA, hemagglutinin.

doxycycline. Plates tested for calcium sensitivity were unbuffered YPD with 200 mM $CaCl_2$ and YPD with 200 mM $CaCl_2$ buffered to pH 7.5. Plates used to test the ability of strains to grow on medium containing glycerol as the sole carbon source were unbuffered yeast extract and peptone (YEP)–2% ethanol–3% glycerol. The ability of strains to respond to challenge with antifungals was tested on YPD (pH 4.0) with 0.025 μg/ml caspofungin, 5 μg/ml fluconazole, or 0.0125 μg/ml amphotericin B. Temperature sensitivity was tested by stamping cells onto unbuffered YPD plates and incubating at 25°C, 30°C, or 37°C for 48 h. Other plates tested were CSM (pH 4.0) plates containing either 1 M NaCl, 200 μg/ml Congo red, or 50 μg/ml calcofluor white. Cells were stamped onto media using a multiblot replicator as described above.

Vacuolar acidification assays. Quinacrine staining was performed to visualize acidified vacuoles as described previously (38), with some modifications. First, cells were grown in unbuffered YPD with or without doxycycline for 24 h to ensure complete turnover of extant Vma3p. Then, cells were reset in fresh unbuffered YPD, with or without doxycycline, and grown to early log phase. Cells were cooled on ice for 1 min and resuspended in 200 μM quinacrine in YPD buffered with 50 mM sodium phosphate (pH 7.6) for 5 min. Cells were washed twice with 100 mM HEPES–50 mM sodium phosphate–2% glucose (pH 7.6) and resuspended in the same solution. Cells were visualized via differential interference contrast (DIC) and fluorescence microscopy. In order to quantify the vacuolar pH, cells were stained with 2′-7′-bis-(2-carboxyethyl)-5-(and-6)-carboxyfluorescein (BCECF)-acetoxymethyl ester (AM) (from Invitrogen), as described previously (24).

V-ATPase assembly and activity assays. Starter cultures were grown for 6 to 8 h in unbuffered YPD with and without doxycycline. Vacuoles were prepared by resetting cells in YPD (pH 4.0) with and without doxycycline and growing to an OD_{600} of 1.0 to 1.5 (approximately 18 h). Vacuolar membranes were purified by Ficoll density gradient centrifugation (39). For Western blots, 80 μg of vacuolar protein was separated by SDS-PAGE and transferred to nitrocellulose overnight at 150 mA. The V_1A subunit was visualized with a 1:1,000 dilution of anti-human V_1A rabbit polyclonal antibody (40); the human V_1A antibody cross-reacts with the *C. albicans* V_1A protein.

To quantify ATP hydrolysis in purified vacuolar vesicles, vacuolar vesicles (15 μg) were added to an enzymatic assay in which the rate of ATP hydrolysis is coupled to the oxidation of NADH, measured as a loss of A_{340} over time (41). Proton transport of purified vacuolar vesicles (30 μg) was measured via quenching of 1 μM 9-amino-6-chloro-2-methoxyacridine (ACMA) upon the addition of 0.5 mM ATP–1 mM $MgSO_4$ (MgATP) as described previously (42, 43). Fluorescence at 410-nm excitation/490-nm emission was monitored for 1 min prior to MgATP addition and for an

TABLE 2 Primer sequences used in this study

Primer	Primer sequence (5′–3′)	Source
VMA3-5DRb	TATAATAAATTAAATTAATAGGTAACAATTGAGATTCGATTACAATGAACGCCCACTTGG GAACAACAACGTTTTCCCAGTCACGACGTT	This study
VMA3-3DRb	TGAAAATATGAAAGACTATAGTAAGTAGGGCCATATGACCATTGTTGATGGATATCAGCT CCCACTTTTCTGTGGAATTGTGAGCGGATA	This study
VMA3-5Det	AATGCGATGAGACTTTGCAT	This study
VMA3-3Det	GACTGGCGAAAACTAGTGGG	This study
VMA3-5SB	CCCACTAGTTTTCGCCAGTC	This study
VMA3-3SB	TGAGCATTCACAGTACCAGG	This study
tetVMA3-5DR	TCAAGTTTTGGGATTGTTGCACAACATCTAAGATTTGTTGAGTCAAAGCAGAATCAGC CAATGGGAAAGCGTAATACGACTCACTATAGGG	This study
tetVMA3-3DR	TTCCCTTCTGCAATTGAGTCCATCTGTAATCTAATCAAACAGCAAACATACCATAAATC AGACATATTTTCTAGTTTTCTGAGATAAAGCTG	This study
tetVMA3-5Det	AGCAGCAATAACTGGTCTGG	This study
tetVMA3-3Det	GGTTCCCTTCTGCAATTGAG	This study
tetINS-3Det	CTAGTTTTCTGAGATAAAGCTG	This study
VMA3-5Sblt	TGAGGTGACAGAAGCAGCAA	This study
VMA3-3Sblt	CAACAGATAAACCAGCACCC	This study
RT-VMA3-5Det	GCCGGTATTATTGCCATTTA	This study
RT-VMA3-3Det	ACGTCTTGAGAAGCTCTTG	This study
ENO-SF	TTGATAATTCAGGAATATTACAAC	Milne et al. (48)
uUME6-5DR	CCTGTTATTATAATCAAGGTTAGATATATAATTGGCTCATTATTGCTTTGCTTTACATA ATTGGTGATAGCGTTAGTATCGAATCGACAGC	This study
uUME6-3DR	TTGTATCTTCTCCATAAGGCGAATTTGGTGCTGAAGAAGTTGAATCGGGTGTAACCATA TGGGTAATCATTGTTGTAATATTCCTGAATTATC	This study
UME6-5Det	TCAATTAGAAACCAACAGAGG	This study
UME6-3Det	CAGCAGCACTAACACTGACAC	This study
UME6-3Det2	GAGCCAGATGTAAATATGGAG	This study
uRIM8-5DR	CATCAGGTGAAAGTGTATTGCTTAAAGAGCCCACCTTCCCACACCCATAGTTGTAAGT AGGGCAAATAATCGTTAGTATCGAATCGACAGC	This study
uRIM8-3DR	TTGAATGGAAATGGGCGGAGTCGTTAAATAGTTTGGGGGTGGGTAGTATTTTTGATAC TGCTCGTCTCATTGTTGTAATATTCCTGAATTATC	This study
RIM8-5Det	CTACACTCAACCTGTTCCTAG	This study
RIM8-3Det	TAGCGCGTGCATCAACATCAG	This study
RIM8-3Det2	TTCTCCTGGTAACCAGACCT	This study
uCST20-5DR	GACAATCCTCACTTTAAGTCTAACGTATATACGCGTACACCATCTTATACTCCACAT ACATATTGGATTCCGTTAGTATCGAATCGACAGC	This study
uCST20-3DR	GTAGATGAGAAGACTCATTTGGATCTGTTATTGATGTTTGTGTAGGATTGTTCTCTGAA AGTATGCTCATTGTTGTAATATTCCTGAATTATC	This study
CST20-5Det	GTAGTTTGTTAGTAGCGGGTCT	This study
CST20-3Det	AGTGGCTATTCAGACCTGAGT	This study
CST20-3Det2	TGATTCTGGATTGCTCTCGT	This study
uMDS3-5DR	TCTTGAGACTTTTTAACCACTAAGACTTGTGGGTTATATAATAGCAGTTCACATTTGTA GCAAATCTAGACGTTAGTATCGAATCGACAGC	This study
uMDS3-3DR	GATCATCCTTTTCGGTGGGGGGTAATTGTAGACTGTAACAGGCGCTTGCTGTAGGT ATTAACGTAGACATTGTTGTAATATTCCTGAATTATC	This study
MDS3-5Det	GCTTCCTCCTCCCATATCCTC	This study
MDS3-3Det	TGTCGCTGCTACTGTCTGTCA	This study
MDS3-3Det2	CAGGGATGGTGTAGTTGAGT	This study
uEFG1-5DR	TAACATTTAATTTATATTCCAAGAGTTAATTGATTAAACAACTTGGTCCAAGAATTCAT TACCAGGCGTGCGTTAGTATCGAATCGACAGC	This study
uEFG1-3DR	TTTGCTGGGGCATACCGTTATTGTAATTTCCGTTCATTTGATTGTAATAGGGTATAGAAT ACGTTGACATTGTTGTAATATTCCTGAATTATC	This study
EFG1-5Det	CCTTTGTGTCCCTTGCATAC	This study
EFG1-3Det	GCAACAGTGCTAGCTGATTG	This study
EFG1-3Det2	GTTGTTGCATTGTCGATACA	This study

additional 40 s after. Proton transport was calculated as the change in fluorescence for the first 15 s following MgATP addition. For both assays, the V-ATPase inhibitor concanamycin A (100 nM) was used to assess V-ATPase-specific activity.

Vacuolar morphology. For all vacuolar staining, doxycycline was added to the appropriate treatments upon each medium change. Cells were visualized via DIC and fluorescence microscopy. To simultaneously stain vacuoles with FM4-64 [*N*-(3-triethylammoniumpropyl)-4-(6-(4-(diethylamino)phenyl)hexatrienyl) pyridinium dibromide] and CMAC (7-amino-4-chloromethyl coumarin), cells were grown in unbuffered YPD for 24 h in the presence or absence of doxycycline. Then, cells were reset in fresh unbuffered YPD with or without doxycycline and grown to

early log phase. Cells were resuspended to an OD_{600} of 2 to 4 in unbuffered YPD with 40 μM FM4-64, incubated for 15 min at 30°C, and then reset in fresh unbuffered YPD and incubated for 45 min at 30°C. Next, cells were resuspended to an OD_{600} of 0.1 in 10 mM HEPES–5% glucose (pH 7.4). CMAC was added to a concentration of 100 μM, and cells were incubated at room temperature for 15 min and examined via microscopy using Texas Red (FM4-64) and 4′,6-diamidino-2-phenylindole (DAPI) (CMAC) filters. To create a three-dimensional (3D) image of the vacuole, FM4-64 staining was completed as previously described (44), except that prior to staining, cells were grown for 24 h in unbuffered YPD with or without doxycycline to ensure complete turnover of Vma3p. A Zeiss Apotome system was used for capturing Z-stack images. 3D image assembly was completed using AxioVision 4.7 software (Zeiss).

Secretion and filamentation assays. Secretion was assessed on solid media: extracellular protease secretion was assayed on unbuffered bovine serum albumin (BSA) plates (45), and lipase secretion was assayed on unbuffered YNB plus 2.5% Tween 80 plates (46). All plates were prepared with and without 20 μg/ml doxycycline. First, cells were grown in YPD with or without doxycycline for 24 h. Then, 3 μl cells were spotted onto plates. BSA plates were incubated at 30°C for 48 h, and Tween 80 plates were incubated at 37°C for 5 days.

Filamentation was assessed on solid and in liquid media. Solid media tested were YPD with 10% fetal calf serum (FCS), medium 199 supplemented with L-glutamine, Spider medium as previously described (47), and RPMI–L-glutamine. All but Spider medium were prepared with 2% (wt/vol) agar; Spider medium was prepared with 1.35% (wt/vol) agar. Filamentation assays were completed (i) with all media buffered to pH 4, and (ii) on standard filamentation media, unbuffered YPD plus FCS, unbuffered M199 (pH 7.5), and unbuffered Spider (pH 7.2) agar, and on RPMI agar buffered to pH 7.0 with 165 mM MOPS. All plates were prepared with and without 20 μg/ml doxycycline. Three microliters cells from overnight cultures were spotted to agar plates, and plates were incubated at 37°C for 5 days. Filamentation in liquid medium was tested in RPMI–L-glutamine (pH 4.0) in the presence or absence of doxycycline. Medium was inoculated with cells from overnight cultures to a starting density of 5×10^6 cells/ml. Cells were grown at 37°C with shaking at 200 rpm for 2 to 24 h. Cells were visualized via light microscopy at selected time points. We were unable to assess filamentation in liquid fetal calf serum at pH 4.0 due to denaturing of serum proteins at low pH.

We also assessed the effect of chemical inhibition of *VMA3* on filamentation in the wild-type strain SC5314. Filamentation was tested in RPMI–L-glutamine buffered to pH 7.0 with 165 mM MOPS. Medium was inoculated with cells from overnight cultures to a starting density of 5×10^6 cells/ml, and either 10 μM bafilomycin A1 in dimethyl sulfoxide (DMSO) or 5 μM concanamycin A in DMSO was added. The final concentration of DMSO was 3% for bafilomycin A1 and 1% for concanamycin A; therefore, to eliminate the possibility of DMSO effects on filamentation, a 1% DMSO-only control was used. Cells were grown at 37°C with shaking at 200 rpm for 2 to 24 h and were visualized via light microscopy at selected time points.

Overexpression of positive regulators of filamentation. A PCR-based transformation method using nourseothricin as a positive selection marker was used to overexpress *RIM8*, *MDS3*, *UME6*, *EFG1*, or *CST20* by inserting the *ENO1* promoter directly upstream of each gene (48) in the tetR-*VMA3* strain. The genotype of the five resulting strains, listed in Table 1, was tetR-*VMA3*+P_{ENO1}-*RIM8*, tetR-*VMA3*+P_{ENO1}-*MDS3*, tetR-*VMA3*+P_{ENO1}-*UME6*, tetR-*VMA3*+P_{ENO1}-*EFG1*, and tetR-*VMA3*+P_{ENO1}-*CST20*. Amplicons for transformation were generated via PCR using the primers shown in Table 2 and the plasmid pNAT1-ENO1 (from S. Bates, University of Exeter). *C. albicans* tetR-*VMA3* cells were transformed using the lithium acetate method, with a 4-h growth step in YPD added after heat shocking the cells in order to allow integration and translation of the *NAT1* gene before exposing the cells to nourseothricin, as described previously (48). Correct integration of the PCR amplicons was confirmed by allele-specific PCR using one primer inside the amplicon (ENO-SF) (Table 2) and one primer within the open reading frame of the gene targeted for overexpression (Table 2). Integration was further confirmed using an alternative allele-specific PCR with up- and downstream primers flanking the region targeted for insertion (Table 2). Then, tetR-*VMA3*+P_{ENO1}-*RIM8*, -*MDS3*, -*UME6*, -*EFG1*, or -*CST20* cells were spotted to filamentation-inducing media as described above to determine whether overexpression of these positive regulators of filamentation would rescue the filamentation defect observed in the tetR-*VMA3* strain in the presence of doxycycline. The tetR-*VMA3*+P_{ENO1}-*UME6* strain was further investigated; first, tetR-*VMA3* and tetR-*VMA3*+P_{ENO1}-*UME6* cells were grown in unbuffered YPD with or without doxycycline for 24 h. Then, cells were washed twice in 1× PBS and resuspended in PBS. Cells in PBS were visualized via light microscopy at 0 h. Finally, cells were seeded in unbuffered YPD plus 10% FCS to a concentration of 5×10^6 cells per ml and incubated at 37°C, 200 rpm, for 24 h, with visualization via light microscopy at selected time points.

Biofilm formation. Biofilm formation was tested using the XTT-reduction assay as previously described (37). Biofilms were formed in RPMI–L-glutamine buffered to pH 4.0 to 8.5. Each treatment was performed in quadruplicate, and each experiment was repeated twice.

Macrophage killing assays. The *in vitro* model of macrophage infection was performed as previously described (12). The J774A.1 murine macrophage cell line was purchased from ATCC. Macrophage cells were grown in unbuffered high-glucose Dulbecco's modified Eagle medium (DMEM) supplemented with 10% FCS at 37°C with 5% CO_2 for 72 h. Next, fresh unbuffered DMEM plus 10% FCS was seeded with 2×10^5 macrophage cells/ml, and 0.75 ml of this solution was used to seed Lab-Tek chambered slides (Nalge-Nunc). The slides were incubated at 37°C, 5% CO_2, overnight. Spent medium was removed, and adherent macrophage cells were washed twice with PBS. Overnight cultures of *C. albicans* strains were washed three times in PBS, and *C. albicans* cells were added to unbuffered DMEM plus 10%FCS, with or without doxycycline, to a multiplicity of infection (MOI) of 2. *C. albicans* cells were coincubated with adherent macrophage cells overnight at 37°C with 5% CO_2. Then, cells were washed twice with PBS, and macrophage viability was assessed using the Invitrogen Live/Dead viability/cytotoxicity kit, following the manufacturer's instructions. Live macrophages from 12 separate fields of each chamber were counted, and the results were analyzed for statistical differences using one-way analysis of variance (ANOVA), followed by the Tukey's multiple-comparison test (GraphPad Prism 5.01). The experiment was performed independently three times, and a representative experiment is presented.

RESULTS

Genetic analysis and disruption of *VMA3*. Vma3p is a highly conserved protein (49) largely composed of hydrophobic residues. A BLASTp search of the *Candida* genome database using the *S. cerevisiae* Vma3p sequence as a query revealed a single 161-amino-acid predicted protein with 87.5% identity and 94.4% similarity to *S. cerevisiae* Vma3p. Hydrophobic residues such as isoleucine, phenylalanine, valine, and leucine comprise 39% of *C. albicans* and 40% of *S. cerevisiae* Vma3p. Transmembrane structure prediction of Vma3p using the software program Phobius (50) revealed four transmembrane domains in the open reading frame which are present at identical locations in *C. albicans* and *S. cerevisiae* Vma3p. Given its high degree of structural conservation, we anticipated that genetic deletion of *VMA3* in *C. albicans* would mimic findings for *S. cerevisiae* in that it should prevent V_o assembly, eliminate all V-ATPase function, and allow us to assess the contribution of *VMA3* and V-ATPase function to *C. albicans* physiology and virulence-related phenotypes.

Therefore, we attempted to construct a *vma3*Δ null mutant in *C. albicans*. Because *vma* mutants in *S. cerevisiae* and *C. albicans* grow poorly on alkaline media, we buffered all selective medium

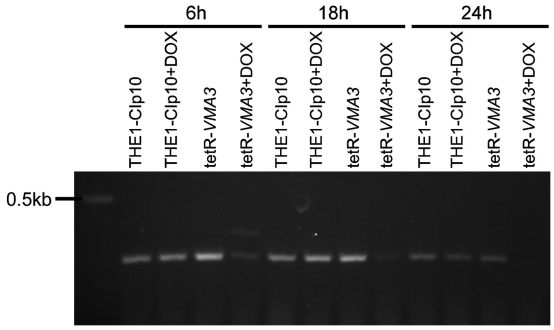

FIG 1 RT-PCR analysis of *VMA3* expression. RNA was extracted from THE1-CIp10 and tetR-*VMA3* cells after 6, 18, and 24 h of incubation in unbuffered YPD with doxycycline (DOX). For comparison, RNA was also extracted from THE1-CIp10 and tetR-*VMA3* cells incubated for 6, 18, and 24 h in unbuffered YPD without doxycycline. Reverse transcriptase PCR (RT-PCR) was used to amplify the 300-bp *VMA3* transcript using the primers RT-VMA3-5Det and RT-VMA3-3Det. After 6 and 18 h of treatment with doxycycline, the *VMA3* transcript was still present in the tetR-*VMA3* strain. After 24 h of treatment with doxycycline, the *VMA3* gene was completely repressed.

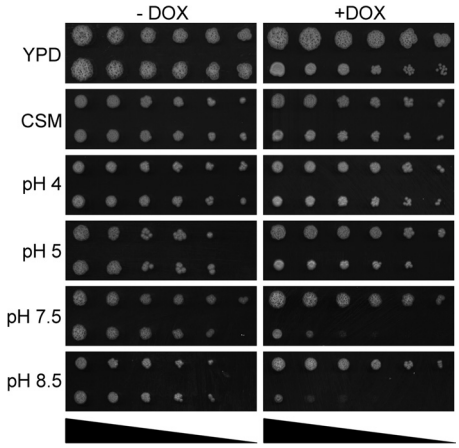

FIG 2 Growth on unbuffered YPD, unbuffered complete synthetic media (CSM), and CSM buffered to pH 4 to pH 8.5 at 30°C. The triangle at the bottom of each column indicates decreasing cell densities (1.0×10^8, 2.0×10^7, 4.0×10^6, 8.0×10^5, 1.6×10^5, and 3.2×10^4 cells/ml, from left to right). In both columns, the top row is the THE1-CIp10 strain, and the bottom row is the tetR-*VMA3* strain. In the presence of doxycycline, the tetR-*VMA3* strain exhibits poor growth at pH 7.5 and pH 8.5.

plates to either pH 4.0 or 5.0 to assist in the selection for positive transformants. One allele of *VMA3* was readily deleted in the BWP17 background using the PCR-based "mini-Urablaster" cassette (31) to generate a *VMA3*/*vma3*Δ::*dpl200-URA3-dpl200* strain. However, in our hands, we were unable to recover second-allele deletion strains at pH 4.0 to pH 5.0 or on unbuffered medium. Therefore, we constructed a conditional *VMA3* mutant, the tetR-*VMA3* strain, using a tetracycline-repressible system (34, 35) in which *VMA3* expression is suppressed in the presence of doxycycline. We used THE1-CIp10, a strain from the THE1 background in which the *URA3* gene has been integrated into the genome, as an additional control (14). Strain construction was confirmed via Southern blot analysis (see Fig. S1 in the supplemental material) and RT-PCR (Fig. 1). RT-PCR analysis indicated that in the presence of doxycycline, the *VMA3* transcript was absent in the tetR-*VMA3* strain after 24 h (Fig. 1). The *VMA3* transcript was present in the tetR-*VMA3* strain in the absence of doxycycline and in the THE1-CIp10 strain both with and without doxycycline (Fig. 1). After 6 and 18 h of treatment with doxycycline, the *VMA3* transcript was still present in the tetR-*VMA3* strain. In all subsequent experiments, all strains were grown for 24 h in the presence or absence of doxycycline prior to the start of the experiment to ensure complete disruption of *VMA3*.

The tetR-*VMA3* strain exhibits the *vma* phenotype. Cells carrying genetic disruptions of V-ATPase subunits develop the *vma* phenotype in *S. cerevisiae*, characterized by pH-conditional lethality (16). To test for pH-dependent growth, tetR-*VMA3* cells were spotted on medium adjusted to a broad pH range (pH 4.0 to 8.5). tetR-*VMA3* strain growth was comparable to that of the THE1-CIp10 control strain under derepressing conditions (Fig. 2). After addition of doxycycline to repress *VMA3* expression, tetR-*VMA3* strain growth was decreased at an alkaline pH (pH 7.5 and pH 8.5) (Fig. 2) but not at an acidic pH (pH 4.0 and pH 5.0) (Fig. 2). The *vma* phenotype was also observed in liquid CSM buffered to pH 4 to 8.5 (data not shown). The tetR-*VMA3* cells grew at nearly wild-type levels on nonbuffered YPD and at wild-type levels on CSM under derepressing and repressing conditions (Fig. 2), likely due to acidification of the surrounding medium or of key cellular components. This phenotype has previously been observed in *S. cerevisiae vma* mutants (26).

***VMA3* is involved in stress responses.** The *S. cerevisiae vma3*Δ mutant grows poorly on media containing high concentrations of calcium or on nonfermentable carbon sources (17). It also exhibits increased cold sensitivity (51) and reduced resistance to a variety of stress conditions (16). We thus plated *C. albicans* tetR-*VMA3* cells after 24 h of growth in unbuffered YPD with and without doxycycline on the following: (i) CSM plus 200 mM $CaCl_2$, both unbuffered and buffered to pH 7.5, (ii) unbuffered YEP plus 2% glycerol as the sole carbon source, or (iii) CSM, pH 4, containing the antifungals caspofungin, fluconazole, and amphotericin B. Repression of *C. albicans VMA3* expression significantly reduced tetR-*VMA3* growth under most conditions (Fig. 3A). Notably, tetR-*VMA3* cells had increased sensitivity to caspofungin (0.025 μg/ml) but did not have increased sensitivity to fluconazole (5 μg/ml) and had modestly increased sensitivity to amphotericin B (0.0125 μg/ml) (Fig. 3A). The dependence of V-ATPase function on ergosterol has been elucidated previously (52). Finally, we tested the ability of the tetR-*VMA3* strain to grow at various temperatures after 24 h of growth in unbuffered YPD with and without doxycycline. Like *S. cerevisiae vma*Δ mutants, the tetR-*VMA3* strain showed enhanced sensitivity to lower temperatures under repressing conditions (Fig. 3B). tetR-*VMA3* growth was also tested on medium containing 1.5 M NaCl, 50 μg/ml calcofluor white, or 200 μg/ml Congo red; no difference in growth compared to that of the wild type was observed (data not shown).

***VMA3* is necessary for vacuolar acidification.** V-ATPase proton transport acidifies the vacuolar lumen, and we anticipated that the tetR-*VMA3* vacuolar pH would be altered when *VMA3* was repressed. We stained the tetR-*VMA3* strain with quinacrine, a basic dye that accumulates inside acidic compartments, such as the vacuole (44), to determine whether vacuolar acidification was defective. After 24 h of growth in unbuffered YPD, the vacuoles of tetR-*VMA3* cells accumulated quinacrine comparably to results for the THE1-CIp10 wild-type control (Fig. 4A). After 24 h of

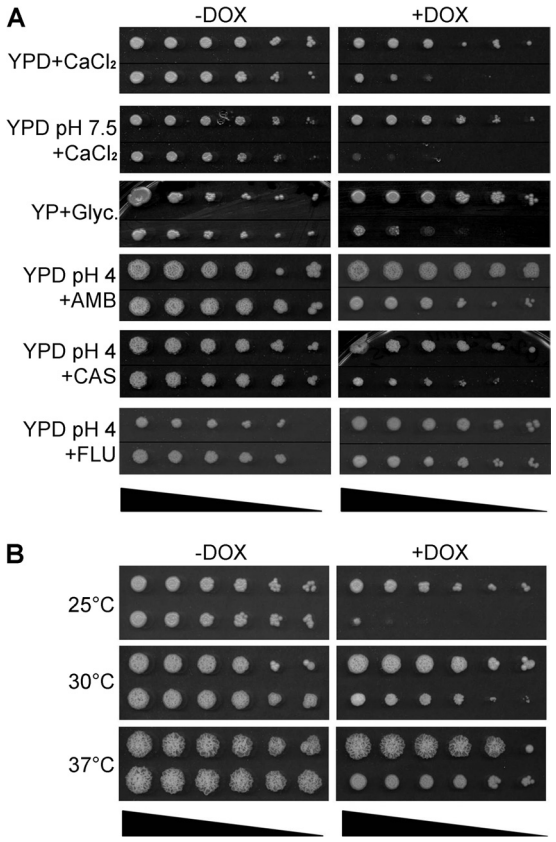

FIG 3 Growth under stress conditions. The triangle at the bottom of each column indicates decreasing cell densities (1.0×10^8, 2.0×10^7, 4.0×10^6, 8.0×10^5, 1.6×10^5, and 3.2×10^4 cells/ml, from left to right). In both columns, the top row is the THE1-CIp10 strain, and the bottom row is the tetR-*VMA3* strain. (A) The abilities of the tetR-*VMA3* strain to respond to high-calcium stress, to use glycerol as a nonfermentable carbon source, and to resist challenge with antifungal agents were tested on agar plates incubated at 30°C. Calcium sensitivity was tested on unbuffered YPD plus 200 mM $CaCl_2$ and on YPD buffered to pH 7.5 plus 200 mM $CaCl_2$. Ability to use glycerol as a nonfermentable carbon source was tested on unbuffered YEP with 2% glycerol and 3% ethanol. Susceptibility to antifungal agents was tested on YPD buffered to pH 4 with 0.0125 μg/ml amphotericin B (AMB), 0.025 μg/ml caspofungin (CAS), or 5 μg/ml fluconazole (FLU) added. Under repressing conditions, the tetR-*VMA3* strain grows poorly on medium containing high concentrations of calcium, glycerol, or caspofungin. (B) tetR-*VMA3* strain growth at various temperatures was tested on unbuffered YPD plates incubated at 25°C, 30°C, or 37°C. Under repressing conditions, the tetR-*VMA3* strain exhibits increased sensitivity to low temperature (25°C).

growth in unbuffered YPD with doxycycline, tetR-*VMA3* vacuoles did not stain with quinacrine. Fluorometric vacuolar pH measurements using BCECF, a pH-sensitive fluorophore that accumulates in the fungal vacuole (42, 53, 54), validated the results obtained with quinacrine (Fig. 4B). Depletion of Vma3p in the tetR-*VMA3* strain led to vacuolar alkalinization, as indicated by an increase in the vacuolar pH from 6.17 to 6.77 upon repression of *VMA3* expression. Together, these results indicate that Vma3p is necessary for vacuolar acidification in *C. albicans*.

***VMA3* is required for V-ATPase assembly and activity.** The vacuolar alkalinization measured in tetR-*VMA3* cells upon depletion of Vma3p suggests that V-ATPase activity was drastically compromised. To directly establish the effect of *VMA3* suppression on V_oV_1 complex assembly and catalytic activity, we purified vacuolar membrane vesicles from cells grown in unbuffered YPD with and without doxycycline for 24 h by density gradient centrifugation. Western blots using an antibody against the catalytic subunit A of V_1 (V_1A) did not detect theV_1A subunit in vacuolar membrane fractions under repressing conditions (Fig. 5A), indicating that V-ATPase complexes are not assembled. This assembly defect suggests that as in *S. cerevisiae* (23), deletion of the V_oc subunit in *C. albicans* prevents assembly of V_o, and consequently, V_1 cannot assemble at the membrane.

The V_1 domain is the site of ATP hydrolysis in the V-ATPase complex, whereas the V_o domain is the site of proton transport. The lack of intact V-ATPase complex upon depletion of Vma3p is thus predicted to result in a significant reduction in both ATP hydrolysis and proton transport. We measured ATP hydrolysis spectrophotometrically using a coupled enzymatic assay (41), and proton transport was measured fluorometrically using ACMA (42, 43). Both assays were performed in the presence and absence of 100 nM concanamycin A, a specific V-ATPase inhibitor. Under tetR-*VMA3* repression, concanamycin A-sensitive ATP hydrolysis decreased by 88% (Fig. 5B) and proton transport decreased by >99% (Fig. 5C). These results are in agreement with the alkalinization of the vacuoles in the tetR-*VMA3* strain upon addition of doxycycline, as evidenced by both quinacrine and BCECF experiments, and confirm that *VMA3* is required for both ATPase hydrolysis and proton transport by the V-ATPase in *C. albicans*.

Interruption of *VMA3* leads to abnormal vacuolar morphology. Our results indicate that *VMA3* is a fundamental V-ATPase component required for V-ATPase activity and maintenance of vacuolar function in *C. albicans*. We next costained vacuoles with FM4-64 and CMAC to determine if lack of V-ATPase function also altered vacuolar morphology. FM4-64 is a lipophilic dye that is endocytosed and transported to the vacuole, where it stains vacuolar membranes. CMAC is a dye that is thought to passively permeate the cell membrane and accumulate in the vacuolar lumen via the action of glutathione pumps; CMAC accumulation is independent of pH (55). For tetR-*VMA3* cells grown in unbuffered medium under repressing conditions, excessive FM4-64 vacuolar membrane staining coincided with CMAC staining of the lumen, indicating intravacuolar accumulation of endocytosed membranes (Fig. 6A). This phenotype was confirmed by performing Z-stack fluorescence microscopy of FM4-64-stained cells (see Movie S1 in the supplemental material). When treated with doxycycline, tetR-*VMA3* cells contained a single spherical or obloid vacuole containing multiple membrane compartments. In contrast, *S. cerevisiae vma3*Δ cells have a single enlarged vacuole (56). The vacuolar morphology of the tetR-*VMA3* strain after 24 h of growth in unbuffered YPD with and without doxycycline was further assessed using thin-section electron microscopy. The vacuolar morphology of the THE1-CIp10 control strain, both with and without doxycycline, has been studied previously (14). Under repressing conditions, the tetR-*VMA3* strain accumulates folds of vacuolar membrane on the interior of the vacuole (Fig. 6B). We observed single, enlarged vacuoles with interior membrane structures in the majority of cells examined (data not shown), indicative of a vacuolar fission defect (56).

***VMA3* contributes to protease and lipase secretion.** The secretion of degradative enzymes is involved in *C. albicans* pathogenesis (5, 8). We assayed *in vitro* secretion of aspartyl proteases and lipases on unbuffered BSA and unbuffered YNB-Tween 80 media, respectively (Fig. 7). *C. albicans* cells, spotted on medium

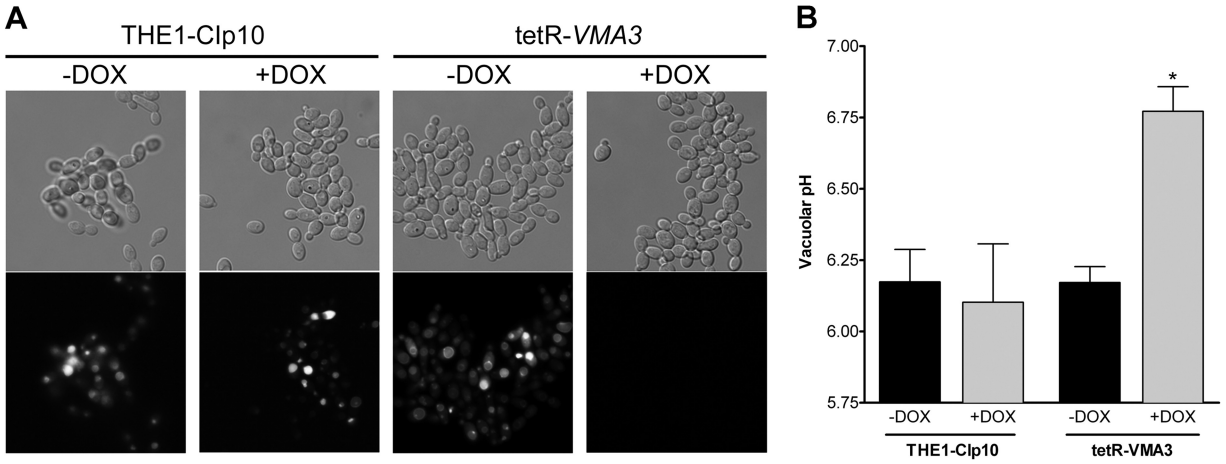

FIG 4 Vacuolar acidification. (A) Quinacrine staining of cells grown in unbuffered YPD with and without doxycycline. Quinacrine accumulates in the vacuole under acidic conditions. Under derepressing conditions, both the THE1-CIp10 and tetR-*VMA3* strains accumulate quinacrine in vacuoles. Under repressing conditions, the tetR-*VMA3* strain does not accumulate quinacrine. (B) BCECF quantification of vacuolar pH in cells grown in unbuffered YPD. After treatment with doxycycline, the tetR-*VMA3* strain exhibits alkalinized vacuoles. Asterisks (*) denotes statistical significance, $P > 0.001$, compared to all other treatments.

containing BSA as the sole nitrogen source, secrete secreted aspartyl proteases (SAPs) that digest the BSA, creating a halo of proteolysis around the colony (45). Like the THE1-CIp10 control strain, the tetR-*VMA3* strain exhibited normal proteolytic activity under derepressing conditions. The addition of doxycycline completely inhibited extracellular proteolytic activity of the tetR-*VMA3* strain (Fig. 7). Similarly, wild-type *C. albicans* cells secrete lipases on YNB-Tween 80 medium, creating a halo of precipitation around the colony. Under repressing conditions, tetR-*VMA3* exhibited decreased lipolytic activity on YNB-Tween 80 agar (Fig. 7).

***VMA3* is required for filamentation.** Since repression of *VMA3* impairs secretion of degradative enzymes involved in pathogenesis, we asked whether other virulence-associated traits are associated with V-ATPase function in *C. albicans*. We assessed *in vitro* filamentation by the tetR-*VMA3* strain on solid and in liquid media buffered to pH 4.0, allowing us to discriminate between filamentation defects and pH-specific growth defects. Under repressing conditions, the tetR-*VMA3* strain did not filament on solid media that are either weak inducers or strong inducers of filamentation (Fig. 8A). In contrast, the tetR-*VMA3* strain grown under nonrepressing conditions produced robust hyphal structures comparable to those of the THE1-CIp10 control strain. We also assessed *in vitro* filamentation of the tetR-*VMA3* strain on standard filamentation media: unbuffered YPD plus FCS, unbuffered M199 (pH 7.5), and unbuffered Spider pH 7.2 agar, as well as RPMI agar buffered to pH 7.0 with 165 mM MOPS. The tetR-*VMA3* strain was also unable to filament under these conditions (data not shown). Under repressing conditions, filamentation of the tetR-*VMA3* strain was dramatically reduced in liquid RPMI (pH 4.0) at 37°C even at 24 h of incubation (Fig. 8B). To further validate the importance of V-ATPase in filamentation, we treated the wild-type *C. albicans* strain SC5314 with specific chemical inhibitors of Vma3p. Concanamycin A and bafilomycin A1 are potent V-ATPase inhibitors that bind specifically to V_oc (Vma3p), blocking rotation of the hydrophobic c ring and preventing proton transport and ATP hydrolysis (57–59). Treatment with concanamycin A (Fig. 8C) and bafilomycin A1 (data not shown) inhibited filamentation. This lack of filamentation upon pharmacological inhibition of V-ATPase further supports the genetic data indicating that V-ATPase-mediated proton transport is essential for *C. albicans* filamentation under a variety of *in vitro* conditions.

The tetR-*VMA3* strain exhibits the *vma* phenotype in biofilms. The adoption of a biofilm lifestyle by *Candida* species on both biotic and abiotic surfaces has been identified as a major factor in their pathogenicity and virulence (60, 61). Therefore, we tested biofilm formation in RPMI (pH 4.0 to 8.5). The THE1-CIp10 control strain formed robust biofilms in RPMI buffered to pH 7.5 or 8.5 and biofilms of lesser metabolic activity in RPMI buffered to pH 4.0 or 5.0 in either the presence or absence of doxycycline (data not shown). At alkaline pH, the tetR-*VMA3* strain exhibited decreased metabolic activity relative to that of the control strain in the presence of doxycycline. However, at acidic pH, the tetR-*VMA3* strain consistently generated metabolic activity similar to that of controls when coincubated with doxycycline, indicating that tetR-*VMA3* exhibits the *vma* growth phenotype in both the biofilm and planktonic states.

The tetR-*VMA3* strain is attenuated in macrophage killing. Phagocytes, such as macrophages and neutrophils, constitute the host's first line of defense against *Candida* infection. After phagocytosis, survival of *C. albicans* within the host is dependent upon induction of phagocyte death (62). We therefore used a murine macrophage killing assay to analyze the contribution of *VMA3* to *in vitro* virulence (Fig. 9). We first tested planktonic growth in unbuffered DMEM over 30 h; there was no significant difference in growth between the tetR-*VMA3* strain with and without doxycycline (data not shown). Next, after 24 h of coincubation in unbuffered DMEM plus 10%FCS, the THE1-CIp10 strain efficiently killed the macrophage cell line, as did the tetR-*VMA3* strain without doxycycline. Upon repression of the *VMA3* gene, the tetR-*VMA3* strain displayed significantly attenuated macrophage killing.

Overexpression of key positive regulators involved in filamentation regulation does not rescue the tetR-*VMA3* filamentation defect. In order to better understand the role of V-ATPase activity in filamentation, we sought to ascertain whether V-

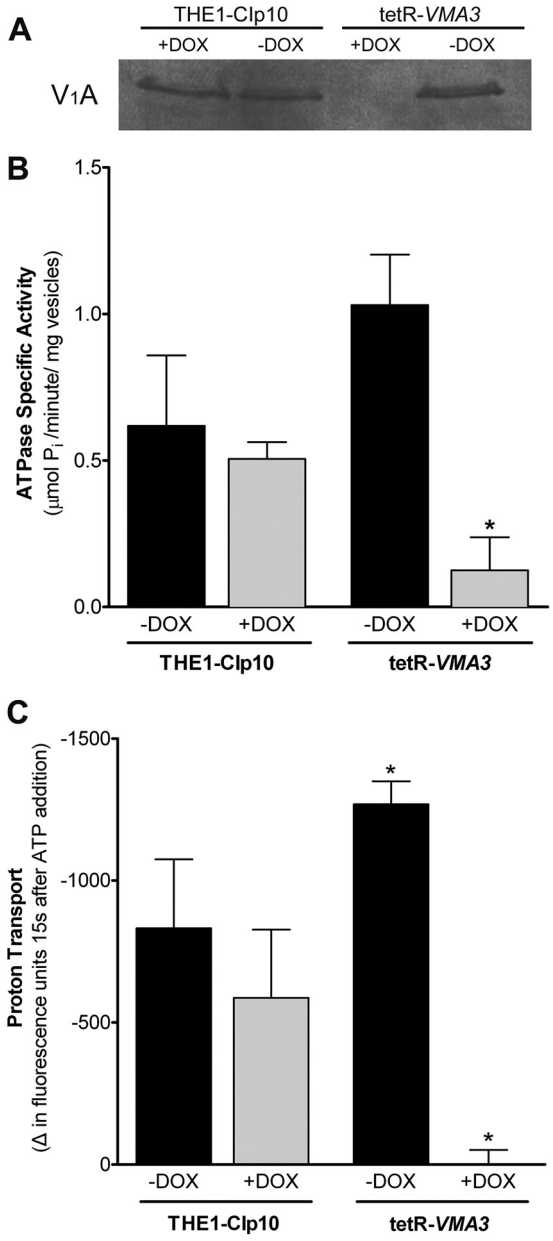

FIG 5 V-ATPase assembly and activity. (A) Western blot using anti-V_1A antibody in vacuolar vesicles purified after 24 h of growth in unbuffered YPD ± doxycycline. Eighty micrograms of vacuolar protein was loaded per lane. The V_1A subunit (Vma1p) is not detected in vacuolar membrane vesicles from the tetR-*VMA3* strain under repressing conditions, indicating that the V-ATPase complex is not properly assembled at the vacuolar membrane. (B) Concanamycin-A-sensitive ATP hydrolysis in vacuolar vesicles purified after 24 h of growth in unbuffered YPD with or without doxycycline. ATPase-specific activity was measured in purified vacuolar vesicles using a spectrophotometric enzyme assay in which ATP hydrolysis is coupled to NADH oxidation. Loss of Vma3p leads to an 88% decrease in concanamycin-A-sensitive ATP hydrolysis. (C) Proton transport in vacuolar vesicles purified after 24 h of growth in unbuffered YPD with or without doxycycline. ATP-dependent proton transport across purified vacuolar membranes was measured via fluorescence quenching of ACMA upon the addition of ATP and $MgSO_4$. Repression of *VMA3* leads to >99% reduction in proton transport activity. Asterisks (*) denote statistical significance, $P < 0.05$, compared to results for all other treatments.

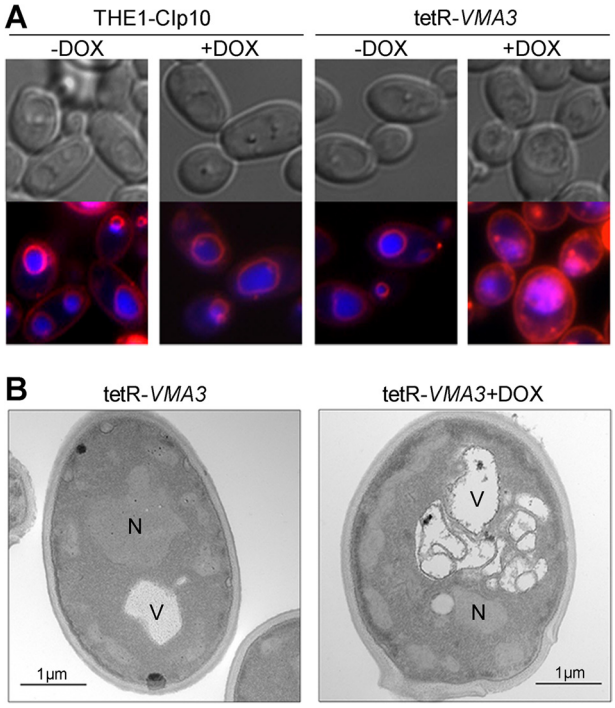

FIG 6 Vacuolar morphology of the tetR-*VMA3* strain. (A) FM4-64 and CMAC double staining of cells grown in unbuffered YPD for 24 h with and without doxycycline. FM4-64 (red) stains vacuolar membranes, and CMAC (blue) stains the vacuolar lumen. Under repressing conditions, FM4-64 and CMAC staining reveal the accumulation of membranous structures on the interior of the vacuole in the tetR-*VMA3* strain. (B) Thin-section electron microscopy of the tetR-*VMA3* strain after 24 h of growth in unbuffered YPD with and without doxycycline. "N" denotes the nucleus, and "V" denotes the vacuole. Under repressing conditions, the tetR-*VMA3* strain displays aberrant vacuolar ultrastructure, indicated by enlarged vacuoles with inclusions of vacuolar membrane on the interior of the vacuole.

ATPase activity is an absolute requirement for filamentation or if the severe filamentation defect in the tetR-*VMA3* strain could be overcome by overexpression of positive transcriptional regulators of filamentation. Thus, we generated strains that overexpressed

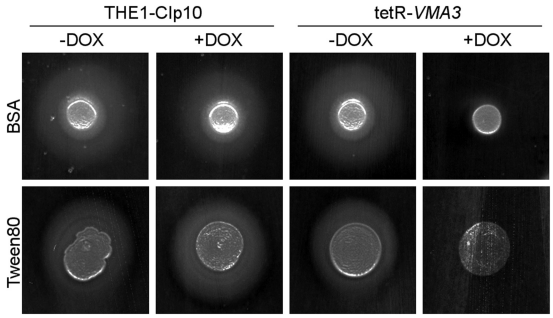

FIG 7 Secretion on BSA and Tween 80 agar. Cells were grown for 24 h in unbuffered YPD with and without doxycycline. Then, secreted aspartyl protease (Sap) secretion was assayed on unbuffered YNB-BSA agar plates (72 h at 30°C), and lipase secretion was determined on unbuffered Tween 80 agar plates (120 h at 37°C). When grown under derepressing conditions, the tetR-*VMA3* strain secretes aspartyl proteases and lipases at levels comparable to those for THE1-CIp10, evidenced by halos of clearance surrounding the colony. When grown under repressing conditions, the tetR-*VMA3* strain exhibits dramatically reduced Sap and lipase secretion.

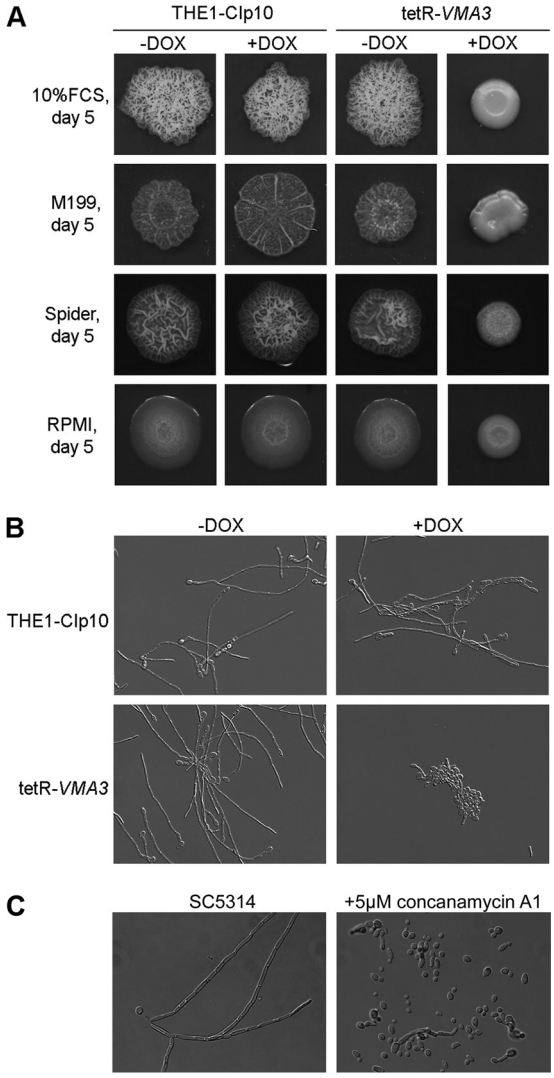

FIG 8 Filamentation on hypha-inducing media. (A) Filamentation on YPD plus 10% FCS, M199, Spider, and RPMI agar plates buffered to pH 4. Cells were grown for 24 h in unbuffered YPD with and without doxycycline and then spotted to agar plates and incubated for 5 days at 37°C. When grown under derepressing conditions, the tetR-*VMA3* strain produces filamentous structures comparable to those of the THE1-CIp10 control strain. When grown under repressing conditions, the tetR-*VMA3* strain exhibits dramatically reduced filamentation on all media tested. (B) Filamentation in liquid culture after 24 h of incubation. Strains were grown in RPMI–L-glutamine with and without doxycycline buffered to pH 4 at 37°C, 200 rpm. When grown under derepressing conditions, the THE1-CIp10 and tetR-*VMA3* strains produced hyphae. When grown under repressing conditions, the tetR-*VMA3* strain exhibited substantially decreased hyphal growth. (C) Filamentation by *C. albicans* SC5314 in the presence or absence of 5 μM concanamycin A1, a V-ATPase inhibitor specific to Vma3p. Strains were grown for 24 h in RPMI–L-glutamine buffered to pH 7 at 37°C, 200 rpm. The addition of concanamycin A inhibited wild-type filamentation.

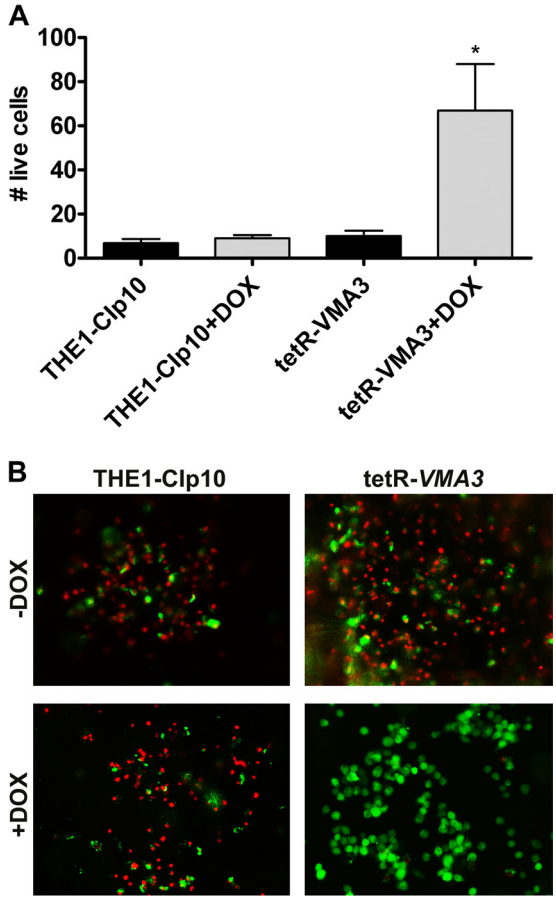

FIG 9 *In vitro* model of macrophage infection. *C. albicans* cells were grown for 24 h in YPD with and without doxycycline before coincubation with macrophage cells in unbuffered DMEM plus 10% FCS at an MOI of 2. (A) Counts of live macrophage cells from 12 separate fields after 24 h of coincubation with *C. albicans* strains. The asterisk denotes statistical significance, $P < 0.01$, compared to all results for other treatments. Each experiment was performed in triplicate; a representative experiment is shown. (B) Live (green) and dead (red) macrophage cells were costained with calcein AM and ethidium bromide homodimer, respectively, and visualized by fluorescence microscopy. Representative images from the 24-h time point are shown.

the positive regulators of filamentation *UME6*, *RIM8*, *CST20*, *MDS3*, and *EFG1* in the tetR-*VMA3* background. Next, we assayed filamentation of these strains on solid filamentation agar with and without doxycycline. Under repressing conditions, overexpression of *RIM8*, *MDS3*, *CST20*, and *EFG1* did not rescue the filamentation defect in the tetR-*VMA3* strain on unbuffered YPD plus 10% FCS agar (Fig. 10A) or on unbuffered M199 (pH 7.5) agar (data not shown).

UME6 is a key regulator of filamentation; overexpression of *UME6* results in constitutive filamentation and can rescue filamentation defects caused by mutations in other genes (63–65), including *RIM8* and *MDS3*, which regulate pH-dependent signaling pathways. In nonrepressing conditions, the P_{ENO1}-*UME6* colony formed robust filaments in a three-dimensional manner, rather than spreading only along the plate's surface (Fig. 10A). The colony was embedded into the agar more deeply and protruded above the surface to a greater extent than the colonies formed by the other strains studied. Therefore, to further analyze the effect of overexpression of *UME6* in the tetR-*VMA3* background, we studied the tetR-*VMA3*+*NAT1*-P_{ENO1}-*UME6* strain in liquid rich medium (unbuffered YPD) and filamentation medium (unbuffered YPD plus 10% FCS). As expected, overexpression of *UME6* led to filamentation in liquid YPD without environmental induction (Fig. 10B). However, upon repression of *VMA3*, the tetR-

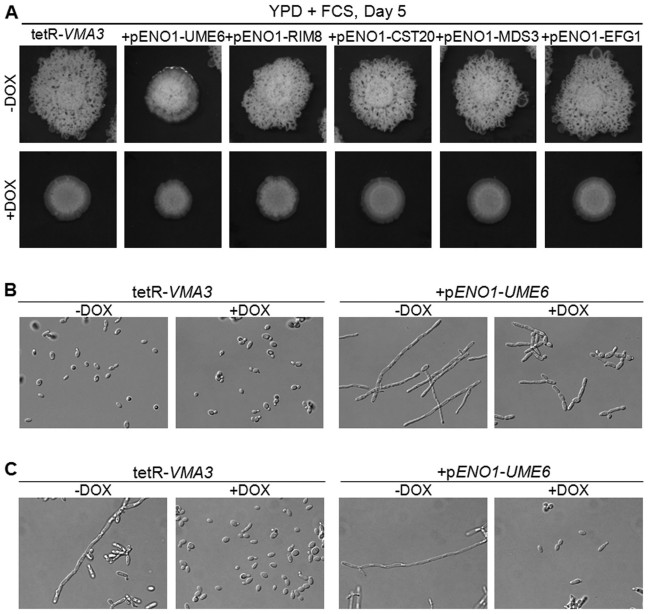

FIG 10 Defective filamentation by the tetR-*VMA3* strain is not rescued by overexpression of key positive regulators of filamentation. (A) Filamentation on unbuffered YPD plus 10% FCS agar plates after incubation at 37°C for 5 days. The addition of doxycycline to hypha-inducing media inhibits filamentation by tetR-*VMA3*. This phenotype is not reversed upon overexpression of Ume6, Rim8, Cst20, Mds3, or Efg1. (B) Cell morphology in non-hypha-inducing conditions (YPD) of the tetR-*VMA3* strain and of the tetR-*VMA3*+P_{ENO1}-*UME6* strain, in which *UME6* is overexpressed in the tetR-*VMA3* background. After 24 h of growth in unbuffered YPD with or without doxycycline, the tetR-*VMA3* strain grows in the yeast form. However, the tetR-*VMA3*+P_{ENO1}-*UME6* strain grows in the hyphal form in the absence of doxycycline and as pseudohyphae in the presence of doxycycline. (C) Filamentation under hypha-inducing conditions (unbuffered YPD plus 10% FCS) after 24 h of incubation at 37°C. Overexpression of *UME6* does not rescue the filamentation defect in the tetR-*VMA3* strain in the presence of doxycycline.

VMA3+*NAT1*-P_{ENO1}-*UME6* strain formed pseudohyphae rather than true hyphae in rich medium (Fig. 10B). We then studied the morphology of the cells in filamentation-inducing medium (unbuffered YPD plus 10% FCS). Despite constitutive filamentation in the absence of doxycycline, in the presence of doxycycline, overexpression of *UME6* did not rescue the tetR-*VMA3* filamentation defect; the majority of cells were observed in yeast rather than pseudohyphal or hyphal form (Fig. 10C). Taken together, these data suggest that V-ATPase activity is a fundamental requirement for filamentation.

DISCUSSION

We have shown that *C. albicans VMA3* is functionally similar to *S. cerevisiae VMA3*. Like *S. cerevisiae vma3*Δ mutants, the *C. albicans* tetR-*VMA3* strain lacks V-ATPase activity and vacuolar acidification upon depletion of Vma3p, and the V_1 subcomplex of the V-ATPase fails to assemble at the vacuolar membrane. The pleiotropic effects associated with loss of V-ATPase activity in both species include an inability to grow on neutral to alkaline media, sensitivity to stress conditions such as high calcium and low temperatures, and growth defects on nonfermentable carbon sources. The centralized role of V-ATPase in stress responses is mainly due to the fact that proton pumping energizes the vacuolar membrane and drives secondary transporters involved in sequestering toxins, such as metal ions and metabolic by-products. For example, previous work in *S. cerevisiae* has suggested that *vma* mutants are able to utilize the aerobic glycerol metabolism pathway but have a defect in the sequestration of one or more by-products of this metabolism (26). Similarly, we showed that the tetR-*VMA3* strain grows poorly on glycerol-containing medium when *VMA3* expression is repressed. Of note, sensitivity of *C. albicans* to high concentrations of calcium and glycerol upon depletion of Vma3p is less severe than that of *S. cerevisiae*. One possible explanation for this difference is that adaptation to extreme environmental changes in the host has increased the ability of *C. albicans* to tolerate various stress conditions relative to that of *S. cerevisiae*.

We are uncertain why we were unable to generate a *C. albicans vma3*Δ null mutant despite the viability of the *S. cerevisiae vma3* null mutant (25–28) and the *C. albicans vma7*Δ null mutant (15). It is possible that locus-specific factors markedly reduced the efficiency of our genomic integrations or that the null mutants were unable to tolerate the stresses induced by lithium acetate transformation, making successful recovery difficult.

We next studied the contribution of *VMA3* to three major *C. albicans* virulence traits: (i) secretion of degradative enzymes, (ii) filamentation, and (iii) biofilm formation. Both the secretion of degradative enzymes and hyphal development are impaired upon depletion of Vma3p. Loss of Vma3p revealed a pH-dependent phenotype in which Vma3p-depleted cells form reduced biofilms compared to those of controls at alkaline pH but form biofilms of mass similar to that for controls at acidic pH. To our knowledge, this is the first demonstration that the *vma* phenotype extends to the biofilm as well as the planktonic form of *C. albicans*. To more directly study the contribution of Vma3p to pathogenesis, we assayed virulence of the tetR-*VMA3* strain in an *in vitro* model of macrophage infection. *In vitro* macrophage killing of Vma3p-deficient cells is significantly attenuated, since macrophage survival increases 7-fold after repressing *VMA3*. This defect in macrophage killing is not simply due to a growth defect, since growth in unbuffered liquid DMEM was normal. Furthermore, macrophage phagosomal pH has been studied extensively; in general, macrophage phagosomal pH becomes acidic (i.e., pH range $>$ 5.0) upon engulfment (66, 67). These data suggest that the V-ATPase complex may play an important role in *C. albicans* pathogenesis and suggest the potential of the V-ATPase as a target for antifungal therapy.

The V-ATPase is important for both vacuolar membrane fission and fusion in *S. cerevisiae*, and *S. cerevisiae vma*Δ mutants exhibit a vacuolar fission defect evidenced by a single enlarged vacuole (56, 68). We have discovered a striking vacuolar fission defect in *C. albicans* upon depletion of Vma3p, as evidenced by the presence of a single enlarged vacuole with an excessive accumulation of membrane. Deletion of *C. albicans VMA7* results in a similar phenotype (15). Vacuolar fission is important for the response to starvation and osmotic stress (56, 69); therefore, defective fission could hinder the ability of the *C. albicans* tetR-*VMA3* strain to respond to environmental stresses. Notably, membrane fission defects are epistatic to membrane fusion defects (56); therefore, the possibility of a hidden membrane fusion defect in V-ATPase mutants cannot be ruled out and is suggested by previous work in both *S. cerevisiae* (56) and *C. albicans* (24). Of note, the cold sensitivity observed in *vma* mutants may be the result of decreased membrane fusion rates; although fusion through the proton pore of the V-ATPase is halted in *vma* mutants, spontaneous mem-

brane fusion does occur at low rates. Decreased temperature may lead to a lethal decrease in the rate of spontaneous membrane fusion as secretion is more fully inhibited (68). We have shown that loss of Vma3p in *C. albicans* results in cold sensitivity. These data suggest a cryptic vacuolar fusion defect in the tetR-*VMA3* strain, and this hypothesis will be tested in future studies. Importantly, defective membrane fusion could partly explain the defect in Sap and lipase secretion observed upon loss of Vma3p, since fusion has been previously linked to secretion (68). Another possible contributor to the accumulation of vacuolar membrane upon *VMA3* repression is fusion of autophagic membrane that cannot be properly degraded due to the inactivity of some degradative proteins at an alkaline vacuolar pH.

The yeast-to-hypha transition is a key element of *C. albicans* pathogenesis (70). Environmental inducers of the yeast-to-hypha transition are compatible with host conditions and include alkaline pH, high temperature, the presence of human serum, and nutrient depletion (71). The response to these environmental triggers requires a highly regulated transcriptional network. The cAMP-PKA pathway, which responds to environmental stimuli, including nitrogen starvation, is one of the major regulatory pathways (72). In this pathway, the adenylyl cyclase Cyr1 utilizes ATP to synthesize cAMP and activate the PKA complex, which then activates filamentation genes, including the transcription factor Efg1, a central regulator of filamentation (73). Maintenance of filamentation after initial hyphal induction is controlled by the transcription factor Ume6 (64, 65, 74). The response to alkaline environmental pH is mediated primarily by the Rim101 signal transduction pathway; this pathway depends on environmental pH sensing, followed by ubiquitinization of Rim8 and processing of the Rim101 transcription factor into an activated form (75–77). A parallel pathway regulated by Mds3 also contributes to filamentation in response to alkaline pH (78, 79). Lastly, the mitogen-activated protein kinase (MAPK) pathway is a lesser contributor to filamentation and includes the protein kinase Cst20, homologous to *S. cerevisiae* Ste20 (47). We overexpressed one positive regulator from each of these five *C. albicans* pathways in the tetR-*VMA3* strain and found that overexpression of *RIM8*, *CST20*, *MDS3*, or *EFG1* does not rescue the filamentation defect in tetR-*VMA3* cells. Overexpression of *UME6* results in partially restored filamentation in YPD (i.e., pseudohyphae) but not under filamentation-inducing conditions, such as YPD plus serum. The role of V-ATPase in filamentation is therefore downstream of these transcriptional regulators or involves independent regulatory mechanisms. These results suggest that V-ATPase activity is a central requirement for filamentation in *C. albicans*.

Loss of *VMA3* more severely inhibits filamentation than loss of the V_oa isoform *VPH1* (24), and this difference has implications for the mechanism of the V-ATPase contribution to filamentation. Interruption of *VMA3* and *VPH1* leads to similar phenotypes, including an ~90% reduction in ATPase-specific activity and an alkalinized vacuole (24). However, loss of *VMA3* expression results in a greater reduction in proton transport levels than *vph1*Δ (99.9% versus 88.0%). The similarity in vacuolar pH between the tetR-*VMA3* strain and the *vph1*Δ strain suggests that protons transported into the vacuole in the *vph1*Δ strain are quickly utilized by downstream membrane pumps and shuttled out of the vacuole. Importantly, after transport into the vacuole by the V-ATPase, protons are utilized in a range of important cellular processes, including protein and membrane trafficking (11, 19). Further studies are needed to clarify which, if any, of these downstream functions are required for filamentation. Membrane trafficking and delivery of cargo proteins is a promising possibility, since the integration of new membrane at the hyphal tip is a key step in germ tube formation (71). Another possible mechanism to explain the filamentation defect is cytosolic acidification. Germ tube formation requires alkalinization of the cytoplasm, a process regulated via the Pma1p plasma membrane proton efflux pump, which maintains a neutral-to-alkaline cytosol and an acidic external environment (53, 80). Pma1p activity and expression are upregulated during filamentation in *C. albicans* (81). In *S. cerevisiae*, the V-ATPase regulates the trafficking and activity of Pma1p, and V-ATPase mutants display an abnormally acidified cytosol (19, 53, 82, 83). If the V-ATPase-Pma1 axis is maintained in *C. albicans*, cytoplasmic alkalinization should be defective upon loss of *VMA3*. In accordance with this model, the differential effect on filamentation upon loss of *VMA3* versus *VPH1* could be due to the presence of Stv1p-containing V-ATPase complexes in the *vph1*Δ strain, leading to partial retention of Pma1p activity (24); detailed studies to define these mechanisms are under way.

The importance of V-ATPase to such diverse cellular processes in *C. albicans*, including processes important for pathogenesis, underscores the potential of the V-ATPase as a drug target. Notably, the antifungal activity of azoles, which inhibit ergosterol biosynthesis, is thought to be partially due to decreased V-ATPase activity in ergosterol-deficient vacuolar membranes (52). Amphotericin B, whose antifungal activity is largely due to ergosterol binding, may also decrease V-ATPase activity (84). Further, naturally occurring compounds have evolved to inhibit V-ATPase, including two highly specific and potent inhibitors isolated from *Streptomyces* species, bafilomycin A1 and concanamycin A (57, 85). Unfortunately, these compounds are poor therapeutic candidates, since they cannot discriminate between mammalian and fungal V-ATPase (86, 87). However, the existence of the fungus-specific V-ATPase subunit c′, which is encoded by *VMA11* and lacks a mammalian homolog, further supports the potential of the V-ATPase as a drug target (17). Future studies will focus on the contribution of *VMA11* and related V-ATPase components to *C. albicans* cell biology and virulence.

ACKNOWLEDGMENTS

We thank Hironobu Nakayama (Suzuka University of Medical Science, Japan) for providing strain THE1 and plasmid p99CAU1, Aaron P. Mitchell (Carnegie Mellon University) for providing plasmid pDDB57, Steven Bates (University of Exeter) for providing plasmid pNAT1-ENO1, and Barbara Hunter (University of Texas Health Science Center at San Antonio) for assistance with transmission electron microscopy. Sequence data for *C. albicans* were obtained from the Stanford DNA Sequencing and Technology Center website at http://www-sequence.stanford.edu/group/candida. Sequencing of *C. albicans* was accomplished with the support of the NIDCR, NIH, and the Burroughs Wellcome Fund.

This work was supported by funding from the Department of Veterans' Affairs (MERIT Award to S.A.L.), Biomedical Research Institute of New Mexico (to S.A.L.), National Institutes of Health Grant 5R01GM086495 (to K.J.P.), UNM IDIP T32 institutional training grant NIH 5 T32 AI007538-13 (to S.M.B.), and National Institutes of Health grant K12GM088021 (to S.M.R.).

REFERENCES

1. **Hidron AI, Edwards JR, Patel J, Horan TC, Sievert DM, Pollock DA, Fridkin SK.** 2008. NHSN annual update: antimicrobial-resistant pathogens associated with healthcare-associated infections: annual summary of

data reported to the National Healthcare Safety Network at the Centers for Disease Control and Prevention, 2006–2007. Infect. Control Hosp. Epidemiol. **29:**996–1011.
2. **Morgan J, Meltzer MI, Plikaytis BD, Sofair AN, Huie-White S, Wilcox S, Harrison LH, Seaberg EC, Hajjeh RA, Teutsch SM.** 2005. Excess mortality, hospital stay, and cost due to candidemia: a case-control study using data from population-based candidemia surveillance. Infect. Control Hosp. Epidemiol. **26:**540–547.
3. **Wisplinghoff H, Bischoff T, Tallent SM, Seifert H, Wenzel RP, Edmond MB.** 2004. Nosocomial bloodstream infections in US hospitals: analysis of 24,179 cases from a prospective nationwide surveillance study. Clin. Infect. Dis. **39:**309–317.
4. **Cowen LE, Steinbach WJ.** 2008. Stress, drugs, and evolution: the role of cellular signaling in fungal drug resistance. Eukaryot. Cell **7:**747–764.
5. **Calderone RA, Fonzi WA.** 2001. Virulence factors of *Candida albicans*. Trends Microbiol. **9:**327–335.
6. **Kumamoto CA, Vinces MD.** 2005. Contributions of hyphae and hypha-co-regulated genes to *Candida albicans* virulence. Cell. Microbiol. **7:**1546–1554.
7. **Lo HJ, Köhler JR, DiDomenico B, Loebenberg D, Cacciapuoti A, Fink GR.** 1997. Nonfilamentous *C. albicans* mutants are avirulent. Cell **90:**939–949.
8. **Naglik JR, Challacombe SJ, Hube B.** 2003. *Candida albicans* secreted aspartyl proteinases in virulence and pathogenesis. Microbiol. Mol. Biol. Rev. **67:**400–428.
9. **Armstrong J.** 2010. Yeast vacuoles: more than a model lysosome. Trends Cell Biol. **20:**580–585.
10. **Banta LM, Robinson JS, Klionsky DJ, Emr SD.** 1988. Organelle assembly in yeast: characterization of yeast mutants defective in vacuolar biogenesis and protein sorting. J. Cell Biol. **107:**1369–1383.
11. **Klionsky DJ, Herman PK, Emr SD.** 1990. The fungal vacuole: composition, function, and biogenesis. Microbiol. Rev. **54:**266–292.
12. **Palmer GE, Kelly MN, Sturtevant JE.** 2005. The *Candida albicans* vacuole is required for differentiation and efficient macrophage killing. Eukaryot. Cell **4:**1677–1686.
13. **Palmer GE.** 2011. Vacuolar trafficking and *Candida albicans* pathogenesis. Commun. Integr. Biol. **4:**240–242.
14. **Bernardo SM, Khalique Z, Kot J, Jones JK, Lee SA.** 2008. *Candida albicans VPS1* contributes to protease secretion, filamentation, and biofilm formation. Fungal Genet. Biol. **45:**861–877.
15. **Poltermann S, Nyugen M, Gunther J, Wendland J, Hartl A, Kunkel W, Zipfel PF, Eck R.** 2005. The putative vacuolar ATPase subunit Vma7p of *Candida albicans* is involved in vacuole acidification, hyphal development and virulence. Microbiology **151:**1645–1655.
16. **Kane PM.** 2006. The where, when, and how of organelle acidification by the yeast vacuolar H+-ATPase. Microbiol. Mol. Biol. Rev. **70:**177–191.
17. **Parra KJ.** 2012. Vacuolar ATPase: a model proton pump for antifungal drug discovery, p 89–100. *In* Tegos G, Mylonakis E (ed), Antimicrobial drug discovery: emerging strategies. CAB International, Wallingford, United Kingdom.
18. **Forster C, Kane PM.** 2000. Cytosolic Ca2+ homeostasis is a constitutive function of the V-ATPase in *Saccharomyces cerevisiae*. J. Biol. Chem. **275:**38245–38253.
19. **Huang C, Chang A.** 2011. pH-dependent cargo sorting from the Golgi. J. Biol. Chem. **286:**10058–10065.
20. **Zhang Y, Rao R.** 2012. The V-ATPase as a target for antifungal drugs. Curr. Protein Pept. Sci. **13:**134–140.
21. **Forgac M.** 1989. Structure and function of vacuolar class of ATP-driven proton pumps. Physiol. Rev. **69:**765–796.
22. **Nelson N, Perzov N, Cohen A, Hagai K, Padler V, Nelson H.** 2000. The cellular biology of proton-motive force generation by V-ATPases. J. Exp. Biol. **203:**89–95.
23. **Graham LA, Flannery AR, Stevens TH.** 2003. Structure and assembly of the yeast V-ATPase. J. Bioenerg. Biomembr. **35:**301–312.
24. **Raines SM, Rane H, Bernardo SM, Binder JL, Lee SA, Parra KJ.** 2013. Deletion of V-ATPase Voa isoforms clarifies the role of vacuolar pH as a determinant of virulence-associated traits in *C. albicans*. J. Biol. Chem. **288:**6190–6201.
25. **Eide DJ, Bridgham JT, Zhao Z, Mattoon JR.** 1993. The vacuolar H(+)-ATPase of *Saccharomyces cerevisiae* is required for efficient copper detoxification, mitochondrial function, and iron metabolism. Mol. Gen. Genet. **241:**447–456.
26. **Ohya Y, Umemoto N, Tanida I, Ohta A, Iida H, Anraku Y.** 1991. Calcium-sensitive cls mutants of *Saccharomyces cerevisiae* showing a Pet(−) phenotype are ascribable to defects of vacuolar membrane H(+)-ATPase activity. J. Biol. Chem. **266:**13971–13977.
27. **Szczypka MS, Zhu Z, Silar P, Thiele DJ.** 1997. *Saccharomyces cerevisiae* mutants altered in vacuole function are defective in copper detoxification and iron-responsive gene transcription. Yeast **13:**1423–1435.
28. **Umemoto N, Yoshihisa T, Hirata R, Anraku Y.** 1990. Roles of the *VMA3* gene product, subunit c of the vacuolar membrane H(+)-ATPase on vacuolar acidification and protein transport. A study with *VMA3*-disrupted mutants of *Saccharomyces cerevisiae*. J. Biol. Chem. **265:**18447–18453.
29. **Katoh K, Toh H.** 2008. Recent developments in the MAFFT multiple sequence alignment program. Brief. Bioinform. **9:**286–298.
30. **Simossis VA, Heringa J.** 2005. PRALINE: a multiple sequence alignment toolbox that integrates homology-extended and secondary structure information. Nucleic Acids Res. **33:**W289–W294.
31. **Wilson RB, Davis D, Enloe BM, Mitchell AP.** 2000. A recyclable *Candida albicans URA3* cassette for PCR product-directed gene disruptions. Yeast **16:**65–70.
32. **Bernardo SM, Lee SA.** 2010. *Candida albicans SUR7* contributes to secretion, biofilm formation, and macrophage killing. BMC Microbiol. **10:**133. doi:10.1186/1471-2180-10-133.
33. **Wilson RB, Davis D, Mitchell AP.** 1999. Rapid hypothesis testing with *Candida albicans* through gene disruption with short homology regions. J. Bacteriol. **181:**1868–1874.
34. **Nakayama H, Mio T, Nagahashi S, Kokado M, Arisawa M, Aoki Y.** 2000. Tetracycline-regulatable system to tightly control gene expression in the pathogenic fungus *Candida albicans*. Infect. Immun. **68:**6712–6719.
35. **Bates S, Hughes HB, Munro CA, Thomas WPH, MacCallum DM, Bertram G, Atrih A, Ferguson MAJ, Brown AJP, Odds FC, Gow NAR.** 2006. Outer chain N-glycans are required for cell wall integrity and virulence of *Candida albicans*. J. Biol. Chem. **281:**90–98.
36. **Ausubel FM, Brent R, Kingston RE, Moore DD, Seidman JG, Smith JA, Struhl K.** 1993.Current protocols in molecular biology. Wiley, New York, NY.
37. **Ramage G, López-Ribot JL.** 2005. Techniques for antifungal susceptibility testing of *Candida albicans* biofilms. Methods Mol. Med. **118:**71–79.
38. **Perzov N, Padler-Karavani V, Nelson H, Nelson N.** 2002. Characterization of yeast V-ATPase mutants lacking Vph1p or Stv1p and the effect on endocytosis. J. Exp. Biol. **205:**1209–1219.
39. **Owegi MA, Pappas DL, Finch MW, Jr, Bilbo SA, Resendiz CA, Jacquemin LJ, Warrier A, Trombley JD, McCulloch KM, Margalef KLM, Mertz MJ, Storms JM, Damin CA, Parra KJ.** 2006. Identification of a domain in the V0 subunit d that is critical for coupling of the yeast vacuolar proton-translocating ATPase. J. Biol. Chem. **281:**30001–30014.
40. **Michel V, Licon-Munoz Y, Trujillo K, Bisoffi M, Parra KJ.** 2013. Inhibitors of vacuolar ATPase proton pumps inhibit human prostate cancer cell invasion and prostate-specific antigen expression and secretion. Int. J. Cancer **132:**E1–E10. doi:10.1002/ijc.27811.
41. **Owegi MA, Carenbauer AL, Wick NM, Brown JF, Terhune KL, Bilbo SA, Weaver RS, Shircliff R, Newcomb N, Parra-Belky KJ.** 2005. Mutational analysis of the stator subunit E of the yeast V-ATPase. J. Biol. Chem. **280:**18393–18402.
42. **Chan C-Y, Prudom C, Raines SM, Charkhzarrin S, Melman SD, De Haro LP, Allen C, Lee SA, Sklar LA, Parra KJ.** 2012. Inhibitors of V-ATPase proton transport reveal uncoupling functions of tether linking cytosolic and membrane domains of V0 subunit a (Vph1p). J. Biol. Chem. **287:**10236–10250.
43. **Forgac M, Cantley L, Wiedenmann B, Altstiel L, Branton D.** 1983. Clathrin-coated vesicles contain an ATP-dependent proton pump. Proc. Natl. Acad. Sci. U. S. A. **80:**1300–1303.
44. **Guthrie C, Fink GR.** 2002. Guide to yeast genetics and molecular and cell biology. Part C. Academic Press, San Diego, CA.
45. **Crandall M, Edwards JE, Jr.** 1987. Segregation of proteinase-negative mutants from heterozygous *Candida albicans*. J. Gen. Microbiol. **133:**2817–2824.
46. **Fu Y, Ibrahim AS, Fonzi W, Zhou X, Ramos CF, Ghannoum MA.** 1997. Cloning and characterization of a gene (*LIP1*) which encodes a lipase from the pathogenic yeast *Candida albicans*. Microbiology **143:**331–340.
47. **Liu H, Köhler J, Fink GR.** 1994. Suppression of hyphal formation in *Candida albicans* by mutation of a *STE12* homolog. Science **266:**1723–1726.
48. **Milne SW, Cheetham J, Lloyd D, Aves S, Bates S.** 2011. Cassettes for

PCR-mediated gene tagging in *Candida albicans* utilizing nourseothricin resistance. Yeast **28:**833–841.
49. **Finnigan GC, Hanson-Smith V, Stevens TH, Thornton JW.** 2012. Evolution of increased complexity in a molecular machine. Nature **481:**360–364.
50. **Käll L, Krogh A, Sonnhammer ELL.** 2005. An HMM posterior decoder for sequence feature prediction that includes homology information. Bioinformatics **21**(Suppl 1):i251–i257.
51. **Oluwatosin YE, Kane PM.** 1998. Mutations in the yeast *KEX2* gene cause a Vma(−)-like phenotype: a possible role for the Kex2 endoprotease in vacuolar acidification. Mol. Cell. Biol. **18:**1534–1543.
52. **Zhang Y-Q, Gamarra S, Garcia-Effron G, Park S, Perlin DS, Rao R.** 2010. Requirement for ergosterol in V-ATPase function underlies antifungal activity of azole drugs. PLoS Pathog. **6:**e1000939. doi:10.1371/journal.ppat.1000939.
53. **Martínez-Muñoz GA, Kane P.** 2008. Vacuolar and plasma membrane proton pumps collaborate to achieve cytosolic pH homeostasis in yeast. J. Biol. Chem. **283:**20309–20319.
54. **Plant PJ, Manolson MF, Grinstein S, Demaurex N.** 1999. Alternative mechanisms of vacuolar acidification in H+-ATPase-deficient yeast. J. Biol. Chem. **274:**37270–37279.
55. **Shoji J, Arioka M, Kitamoto K.** 2006. Vacuolar membrane dynamics in the filamentous fungus *Aspergillus oryzae*. Eukaryot. Cell **5:**411–421.
56. **Baars TL, Petri S, Peters C, Mayer A.** 2007. Role of the V-ATPase in regulation of the vacuolar fission-fusion equilibrium. Mol. Biol. Cell **18:**3873–3882.
57. **Bowman EJ, Graham LA, Stevens TH, Bowman BJ.** 2004. The bafilomycin/concanamycin binding site in subunit c of the V-ATPases from *Neurospora crassa* and *Saccharomyces cerevisiae*. J. Biol. Chem. **279:**33131–33138.
58. **Huss M, Ingenhorst G, König S, Gassel M, Dröse S, Zeeck A, Altendorf K, Wieczorek H.** 2002. Concanamycin A, the specific inhibitor of V-ATPases, binds to the V(o) subunit c. J. Biol. Chem. **277:**40544–40548.
59. **Bowman BJ, Bowman EJ.** 2002. Mutations in subunit C of the vacuolar ATPase confer resistance to bafilomycin and identify a conserved antibiotic binding site. J. Biol. Chem. **277:**3965–3972.
60. **Douglas LJ.** 2003. *Candida* biofilms and their role in infection. Trends Microbiol. **11:**30–36.
61. **Ramage G, Saville SP, Thomas DP, López-Ribot JL.** 2005. *Candida* biofilms: an update. Eukaryot. Cell **4:**633–638.
62. **Miramón P, Kasper L, Hube B.** 2013. Thriving within the host: *Candida* spp. interactions with phagocytic cells. Med. Microbiol. Immunol. **202:**183–195.
63. **Zeidler U, Lettner T, Lassnig C, Müller M, Lajko R, Hintner H, Breitenbach M, Bito A.** 2009. UME6 is a crucial downstream target of other transcriptional regulators of true hyphal development in *Candida albicans*. FEMS Yeast Res. **9:**126–142.
64. **Banerjee M, Thompson DS, Lazzell A, Carlisle PL, Pierce C, Monteagudo C, López-Ribot JL, Kadosh D.** 2008. UME6, a novel filament-specific regulator of *Candida albicans* hyphal extension and virulence. Mol. Biol. Cell **19:**1354–1365.
65. **Carlisle PL, Kadosh D.** 2010. *Candida albicans* Ume6, a filament-specific transcriptional regulator, directs hyphal growth via a pathway involving Hgc1 cyclin-related protein. Eukaryot. Cell **9:**1320–1328.
66. **Ohkuma S, Poole B.** 1978. Fluorescence probe measurement of the intralysosomal pH in living cells and the perturbation of pH by various agents. Proc. Natl. Acad. Sci. U. S. A. **75:**3327–3331.
67. **Tapper H, Sundler R.** 1990. Role of lysosomal and cytosolic pH in the regulation of macrophage lysosomal enzyme secretion. Biochem. J. **272:**407–414.
68. **Peters C, Bayer MJ, Bühler S, Andersen JS, Mann M, Mayer A.** 2001. Trans-complex formation by proteolipid channels in the terminal phase of membrane fusion. Nature **409:**581–588.
69. **Weisman LS.** 2003. Yeast vacuole inheritance and dynamics. Annu. Rev. Genet. **37:**435–460.
70. **Corner BE, Magee PT.** 1997. *Candida* pathogenesis: unravelling the threads of infection. Curr. Biol. **7:**R691–R694.
71. **Sudbery PE.** 2011. Growth of *Candida albicans* hyphae. Nat. Rev. Microbiol. **9:**737–748.
72. **Biswas K, Morschhäuser J.** 2005. The Mep2p ammonium permease controls nitrogen starvation-induced filamentous growth in *Candida albicans*. Mol. Microbiol. **56:**649–669.
73. **Rocha CR, Schröppel K, Harcus D, Marcil A, Dignard D, Taylor BN, Thomas DY, Whiteway M, Leberer E.** 2001. Signaling through adenylyl cyclase is essential for hyphal growth and virulence in the pathogenic fungus *Candida albicans*. Mol. Biol. Cell **12:**3631–3643.
74. **Carlisle PL, Banerjee M, Lazzell A, Monteagudo C, López-Ribot JL, Kadosh D.** 2009. Expression levels of a filament-specific transcriptional regulator are sufficient to determine *Candida albicans* morphology and virulence. Proc. Natl. Acad. Sci. U. S. A. **106:**599–604.
75. **Gomez-Raja J, Davis DA.** 2012. The β-arrestin-like protein Rim8 is hyperphosphorylated and complexes with Rim21 and Rim101 to promote adaptation to neutral-alkaline pH. Eukaryot. Cell **11:**683–693.
76. **Kullas AL, Li M, Davis DA.** 2004. Snf7p, a component of the ESCRT-III protein complex, is an upstream member of the *RIM101* pathway in *Candida albicans*. Eukaryot. Cell **3:**1609–1618.
77. **Wolf JM, Johnson DJ, Chmielewski D, Davis DA.** 2010. The *Candida albicans* ESCRT pathway makes Rim101-dependent and -independent contributions to pathogenesis. Eukaryot. Cell **9:**1203–1215.
78. **Davis DA, Bruno VM, Loza L, Filler SG, Mitchell AP.** 2002. *Candida albicans* Mds3p, a conserved regulator of pH responses and virulence identified through insertional mutagenesis. Genetics **162:**1573–1581.
79. **Zacchi LF, Gomez-Raja J, Davis DA.** 2010. Mds3 regulates morphogenesis in *Candida albicans* through the TOR pathway. Mol. Cell. Biol. **30:**3695–3710.
80. **Stewart E, Gow NA, Bowen DV.** 1988. Cytoplasmic alkalinization during germ tube formation in *Candida albicans*. J. Gen. Microbiol. **134:**1079–1087.
81. **Monk BC, Niimi M, Shepherd MG.** 1993. The *Candida albicans* plasma membrane and H(+)-ATPase during yeast growth and germ tube formation. J. Bacteriol. **175:**5566–5574.
82. **Perzov N, Nelson H, Nelson N.** 2000. Altered distribution of the yeast plasma membrane H+-ATPase as a feature of vacuolar H+-ATPase null mutants. J. Biol. Chem. **275:**40088–40095.
83. **Tarsio M, Zheng H, Smardon AM, Martínez-Muñoz GA, Kane PM.** 2011. Consequences of loss of Vph1 protein-containing vacuolar ATPases (V-ATPases) for overall cellular pH homeostasis. J. Biol. Chem. **286:**28089–28096.
84. **Gray KC, Palacios DS, Dailey I, Endo MM, Uno BE, Wilcock BC, Burke MD.** 2012. Amphotericin primarily kills yeast by simply binding ergosterol. Proc. Natl. Acad. Sci. U. S. A. **109:**2234–2239.
85. **Bowman EJ, Siebers A, Altendorf K.** 1988. Bafilomycins: a class of inhibitors of membrane ATPases from microorganisms, animal cells, and plant cells. Proc. Natl. Acad. Sci. U. S. A. **85:**7972–7976.
86. **Bowman EJ, Bowman BJ.** 2005. V-ATPases as drug targets. J. Bioenerg. Biomembr. **37:**431–435.
87. **Huss M, Wieczorek H.** 2009. Inhibitors of V-ATPases: old and new players. J. Exp. Biol. **212:**341–346.